
Model Collapse Demystified: The Case of Regression

Elvis Dohmatob¹ Yunzhen Feng² Julia Kempe^{2,3,1}

Abstract

In the era of proliferation of large language and image generation models, the phenomenon of “model collapse” refers to the situation whereby as a model is trained recursively on data generated from previous generations of itself over time, its performance degrades until the model eventually becomes completely useless, i.e the model collapses. In this work, we study this phenomenon in the setting of high-dimensional regression and obtain analytic formulae which quantitatively outline this phenomenon in a broad range of regimes. In the special case of polynomial decaying spectral and source conditions, we obtain modified scaling laws which exhibit new crossover phenomena from fast to slow rates. We also propose a simple strategy based on adaptive regularization to mitigate model collapse. Our theoretical results are validated with experiments.

1. Introduction

Model collapse describes the situation where the performance of large language models (LLMs) or large image generators degrade as more and more AI-generated data becomes present in their training dataset (Shumailov et al., 2023). Indeed, in the early stages of the generative AI evolution (e.g the ChatGPT-xyz series of models), there is emerging evidence suggesting that retraining a generative AI model on its own outputs can lead to various anomalies in the model’s later outputs.

This phenomenon has been particularly observed in LLMs, where retraining on their generated content introduces irreparable defects, resulting in what is known as “model collapse”, the production of nonsensical or gibberish output (Shumailov et al., 2023; Bohacek & Farid, 2023). Though several recent works demonstrate facets of this phenomenon *empirically* in various settings (Hataya et al., 2023; Martínez et al., 2023a;b; Bohacek & Farid, 2023; Briesch et al., 2023;

Guo et al., 2023), a theoretical understanding is still missing.

In this work, we initiate a theoretical study of model collapse in the setting of high-dimensional supervised-learning with kernel regression. Kernel methods are popular in machine learning because, despite their simplicity, they define a framework powerful enough to exhibit non-linear features, while remaining in the convex optimization domain. While popular in their own right, kernel methods have made a recent spectacular comeback as proxies for neural networks in different regimes (Belkin et al., 2018), for instance in the infinite-width limit (Neal, 1996; Williams, 1996; Jacot et al., 2018; Lee et al., 2018) or in the lazy regime of training (Chizat et al., 2019). Caponnetto & de Vito (2007) characterize the power-law generalization error of regularized least-squares kernel algorithms, assuming a power-decay spectrum of the kernel (capacity) and of the coefficients of the target function (source). The role of optimization can also be taken into account in this setting (Nitanda & Suzuki, 2021). Source and capacity power decay capture properties of the data and the model that give rise to power law scaling of test error in terms of data set size and model capacity, as empirically observed e.g. in Kaplan et al. (2020); Hoffmann et al. (2022). More recently, scaling laws have been shown for kernel models under the Gaussian design, e.g. in Spigler et al. (2020); Cui et al. (2021; 2022) for regression and Cui et al. (2023) for classification. Rahimi & Recht (2008); Rudi & Rosasco (2017); Maloney et al. (2022) study scaling laws for regression in the random feature (kernel) model. In the nonparametric literature, for example Schmidt-Hieber (2017) and Suzuki (2019) derived the test error scaling of deep neural network in fitting certain target functions and Bordelon et al. (2020) analyzed spectral dependence.

Summary of Main Contributions. Following the rich tradition in prior works outlined above, we study the Gaussian design where the input x is sampled from a multivariate zero-mean Gaussian and labels y are determined by a linear ground truth function with independent label noise as $y = x^\top w_0 + \epsilon$ (we present the linear regression setting for ease, the generalization to the kernel setting is straightforward). At each generation step, an approximation to w_0 is learned from the data, and used to generate new, “fake”/synthetic labels for the next generation. Our main findings can be summarized as follows:

¹Meta FAIR ²Center for Data Science, New York University
³Courant Institute, New York University. Correspondence to: Elvis Dohmatob <dohmatob@meta.com>.

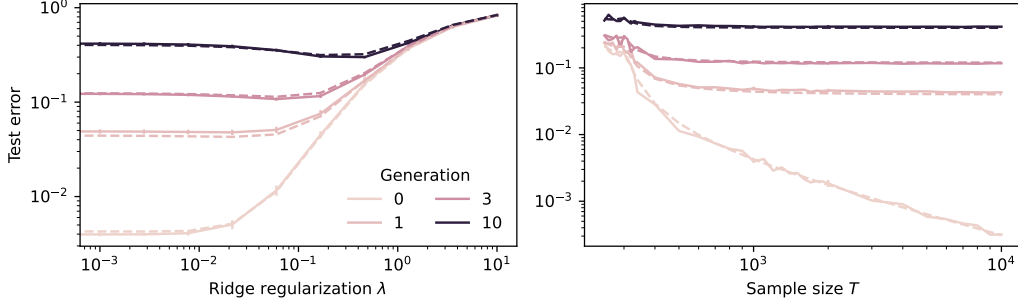


Figure 1. Demystifying model collapse in ridge regression (isotropic covariance spectrum). We show the evolution of test error for different sample size (T), different levels of ridge-regularization (λ), and training data from different generations (n) of fake data. The setup is: input-dimension $d = 300$, sample size for fake data generator $T_0 = 600$, noise levels $\sigma = 0.1$ and $\sigma_0 = 0.2$. **Left plot** is for $T = 1000$ and different values of λ . Notice the U-shape of the curves for large values of n , indicating the existence of a sweet spot (optimal regularization parameter). **Right plot** is for $\lambda = 10^{-3}$ and different values of T . Error bars correspond to uncertainty induced by the data-generating process, over different runs. The broken lines correspond to the theoretical result established in Theorem 4.1.

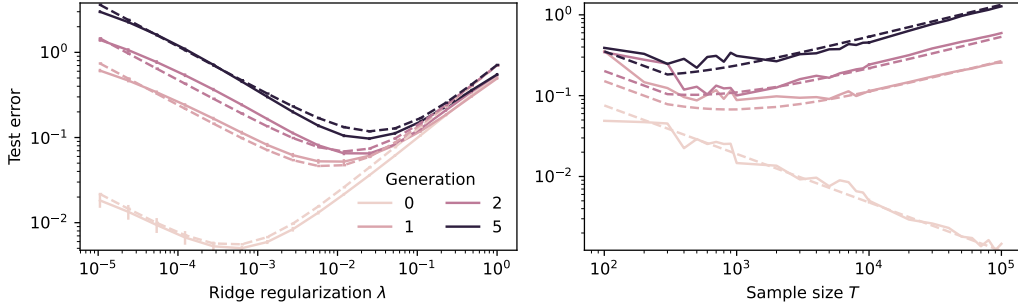


Figure 2. Demystifying model collapse in ridge regression (power-law covariance spectrum). The setup is: $d = 300$, $T_0 = 600$, $\sigma = \sigma_0 = 1$, $\Sigma = \text{diag}(\lambda_1, \dots, \lambda_d)$, where $\lambda_k \propto k^{-2}$. **Left plot** corresponds to $T = 10,000$ and **Right plot** corresponds to adaptive regularization $\lambda = T^{-\ell_{crit}}$, where $\lambda = \lambda(T)$ as proposed in Cui et al. (2022). See Section 6 for details. The broken curves are as predicted by our Theorem 5.2. Though $\ell = \ell_{crit}$ is optimal in classical case, it is not in the setup of model collapse. In fact here, the test error diverges with sample size T . Our theory proposes a corrected value of this exponent which gracefully adapts to synthesized data.

(1) *Exact Characterization of Test Error under Iterative Retraining on Synthesized Data.* In Section 4 (Theorem 4.3), we obtain analytic formulae for test error under the influence of training data with fake l synthesized labels. For n -fold iteration of data-generation, this formula writes

$$E_{test} = E_{test}^{clean} + \Delta Bias + n \times Scaling, \quad (1)$$

where E_{test}^{clean} is the usual test error of the model trained on clean data (not AI-generated). The non-negative term *Scaling* precisely highlights the effects of all the relevant problems parameters like: the feature covariance matrix Σ , sample size T , label noise level in the clean data distribution σ_0^2 , label noise level in the fake data distribution σ^2 , etc. The nonnegative term *$\Delta Bias$* is an increase in bias brought about by the iterative synthetic data generation process. This term disappears if each stage in the process was fitted on sufficiently many samples T_0 compared to the input dimension d (i.e if $T_0 \geq d$). In the case where $T_0 < d$, this term is either a constant or an increasing function of n , depending on whether the design matrix stays the same or is resampled

across different generations. Note that the machine learner has no control over the fake data generation process. It only sees data from a stage n of this process, which is then used to fit a downstream predictor.

A direct consequence of (1) is that, as the number of generations n becomes large, the effect of re-synthesizing will make learning impossible. We note that the multiplicative degradation in scaling with the number of generations n is completely analogous to what has been shown in (Dohmatob et al., 2024) for infinite memory models and their variants and also empirically observed there. See Figures 1 and 3 for an illustration.

(2) *Modified Scaling Laws.* Turning to the special case of power-law spectra of the covariance matrix, which allows to derive test-error scaling laws (Caponnetto & de Vito, 2007; Spigler et al., 2020; Cui et al., 2022; Liang & Rakhlin, 2020), we obtain in Section 5 (see Theorem 5.2) precise new scaling laws of the test error that quantitatively highlight the negative effect of training on synthetically generated data.

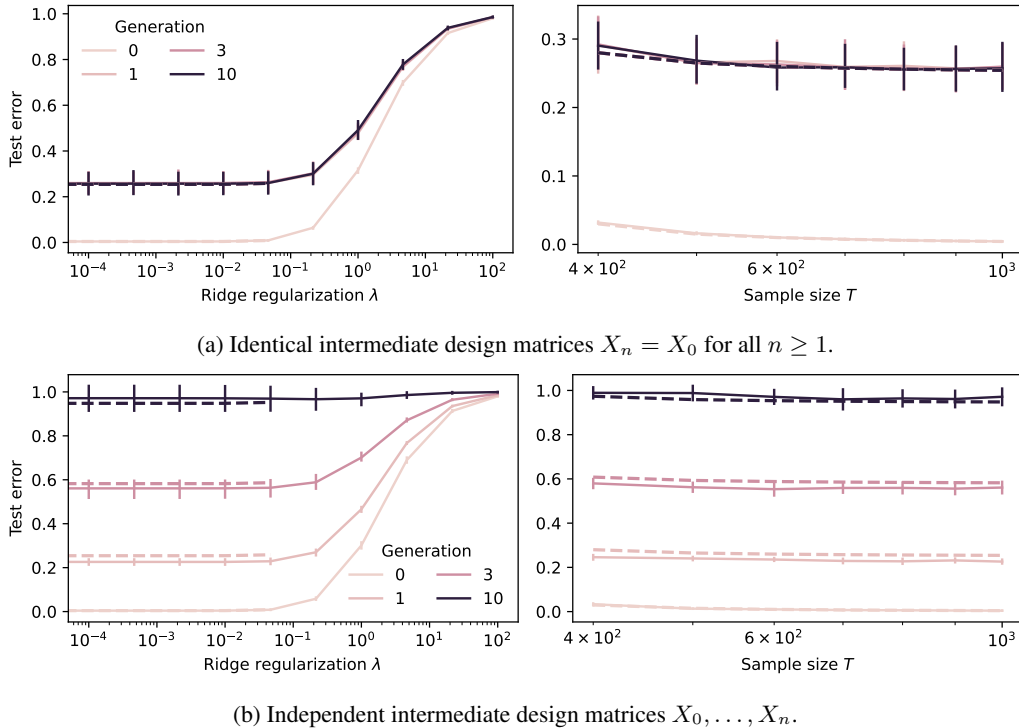


Figure 3. **Model collapse in the case of noiseless over-parametrized synthetic data generator.** Here $d = 300$, the sample sizes for the different versions of the fake data generator are equal, i.e $T_n = T_0 = d/2$ for all n , and noise levels are $\sigma_0 = 0$ and $\sigma = 0.1$. Everything else is as in the setting of Figure 1. Broken lines correspond to the theoretical estimates given in Theorem 4.6. As predicted by our theory, the test error of the model fitted on synthetic data ($n \geq 1$) increases (relative to the baseline $n = 0$, corresponding to training on clean data). The model collapse here, even in the absence of noise ($\sigma_0 = 0$), is due to the fact that the synthetic data-generator does not have access to enough data to capture the true labelling function. **(a)** Importantly, and in accordance to our theory, the amount of model collapse in the case $X_n \equiv X_0$ is due to an increase in bias term of the test error of the model and does not depend on the number of generations n as long as $n \geq 1$. **(b)** In contrast, for the case where the X_n 's are independent, the increase in bias term grows with n , leading to "catastrophic" model collapse (Theorem 4.9).

Further exploiting our analytic estimates, we obtain (Corollary 5.3) the optimal ridge regularization parameter as a function of all the problem parameters (sample size, spectral exponents, strength of fake data-generator, etc.). This new regularization parameter corresponds to a correction of the the value proposed in the classical theory on clean data (Cui et al., 2022), and highlights a novel crossover phenomenon where for an appropriate tuning of the regularization parameter, the effect of training on fake data is a degradation of the fast error rate in the noiseless regime (Cui et al., 2022; Caponnetto & de Vito, 2007) to a much slower error rate which depends on the amount of true data on which the fake data-generator was trained in the first place. On the other hand, a choice of regularization which is optimal for the classical setting (training on real data), might lead to catastrophic failure: the test error diverges. See Figure 2 for an illustration.

2. Review of Literature

Model Collapse. Current LLMs (Devlin et al., 2018; Liu et al., 2019; Brown et al., 2020; Touvron et al., 2023), in-

cluding GPT-4 (Achiam et al., 2023), were trained on predominantly human-generated text; similarly, diffusion models like DALL-E (Ramesh et al., 2021), Stable Diffusion (Rombach et al., 2022), Midjourney (Midjourney, 2023) are trained on web-scale image datasets. Their training corpora already potentially exhaust all the available clean data on the internet. A growing number of synthetic data generated with these increasingly popular models starts to populate the web, often indistinguishable from "real" data. Recent works call attention to the potential dramatic deterioration in the resulting models, an effect referred to as "model collapse" (Shumailov et al., 2023). Several recent works demonstrate facets of this phenomenon *empirically* in various settings (Hataya et al., 2023; Martínez et al., 2023a;b; Bohacek & Farid, 2023; Briesch et al., 2023; Guo et al., 2023). Theoretically, a few works are emerging to analyze the effect of iterative training on self-generated (or mixed) data. Taori & Hashimoto (2023) call attention to *bias* amplification of iterative "data-feedback" loops, also observed in the recommendations systems literature. Shumailov et al. (2023) attribute model collapse to two mechanisms: a finite sampling bias leading to more and more peaked distributions

and function approximation errors, and analyze the (single) Gaussian case. In the context of vision models, Alemohammad et al. (2023) analyze "self-consuming loops" by introducing a sampling bias that narrows the variance of the data at each generation, and provide theoretical analysis for the case of a Gaussian. Bertrand et al. (2023) explore scenarios involving a mix of clean data, representative of the true distribution, and synthesized data from previous iterations of the generator. Their analysis reveals that if the data mix consists exclusively of synthesized data, the generative process is likely to degenerate over time, leading to what they describe as a 'clueless generator'. Conversely, they found that when the proportion of clean data in the mix is sufficiently high, the generator, under certain technical conditions, retains the capability to learn and accurately reflect the true data distribution. Note that such a compounding effect of synthesized data is already reminiscent of our decomposition (1).

Self-Distillation. Importantly, the fake data generation process which is responsible for model collapse should not be confused with self-distillation as formulated in Mobahi et al. (2020) for example. Unlike model collapse, the data generation process in self-distillation actually helps performance of the downstream model. The model has access to training labels from the true data distribution, but decides to fit a model on this data, and then use its outputs as the new labels, iterating this process possibly over severable steps. Thus, self-distillation has control over the data generating process, which is carefully optimized for the next stage training. Specifically, (Mobahi et al., 2020) study self-distillation in the same Gaussian regression model underlying our analysis, but in each distillation generation are able to tune the regularization parameter for downstream performance as a function of the original data labels (with the data being the same at each generation). In the setting of model collapse, there is no control over the data generation process, since it constitutes synthesized data which typically comes from the wide web.

Kernel Ridge Regression with Gaussian Design. This model has been studied by a vast body of works. For example, Richards et al. (2021); Hastie et al. (2022); Bach (2023) analyze the classical bias-variance decomposition of the test error for ridge regression in the high dimensional setting where dataset size and dimension diverge proportionately, using tools from Random Matrix Theory (RMT). In Section 4 we significantly extend this type of analysis to training on iteratively generated synthetic data. This model is also particularly attractive because it allows to analyze an important trade-off: the relative decay of the eigenvalues of the kernel (*capacity*) and the coefficients of the target function in feature space (*source*). Sizeable effort has been dedicated to characterize the influence on the decay rate of the test

error as a function of these two relative decays (aka *power laws*) (Caponnetto & de Vito, 2007; Pillaud-Vivien et al., 2018; Berthier et al., 2020; Richards et al., 2021; Spigler et al., 2020; Cui et al., 2022; 2023). In Section 5 we extend these efforts, in particular based on works of Cui et al. (2021; 2022) which has given a full characterization of all regimes and test error decay that can be observed at the interplay of noise and regularization, characterizing a crossover transition of rates in the noisy setting. Our work uncovers fascinating new effects as a result of iterative training on synthetic data.

3. Theoretical Setup

We now present a setup which is simple enough to be analytically tractable, but rich enough to exhibit a wide range of regimes to illustrate a range of new phenomena that emerge with *model collapse*, described in Section 1 and Section 2. Figure 4 provides a visual representation.

Notations. This manuscript will make use of the following standard notations. The set of integers from 1 through d is denoted $[d]$. Given a variable z (which can be the input dimension d or the sample size T , etc.) the notation $f(z) \lesssim g(z)$ means that $f(z) \leq Cg(z)$ for sufficiently large z and an absolute constant C , while $f(z) \asymp g(z)$ means $f(z) \lesssim g(z) \lesssim f(z)$. For example, $1 + z^2 \asymp \max(1, z^2)$. Further, $f(z) \simeq g(z)$ means $f(z) = (1 + o(1))g(z)$, where $o(1)$ stands for a quantity which tends to zero in the limit $z \rightarrow \infty$. We denote with A^\dagger the Moore-Penrose pseudo-inverse any matrix A , and by $\|A\|_{op}$ is operator norm. Finally, we denote the trace of a square matrix A by $\text{tr } A$, while $\|u\|_A := \sqrt{u^\top Au}$ is the Mahalanobis norm induced by a positive-definite matrix A .

Data Distribution & Fake Data-Generation Process. Consider the distribution $P_{\Sigma, w_0, \sigma^2}$ on $\mathbb{R}^d \times \mathbb{R}$ given by

Data Distribution.

$$\left. \begin{aligned} \text{(Input)} \quad &x \sim N(0, \Sigma), \\ \text{(Noise)} \quad &\epsilon \sim N(0, \sigma^2), \text{ independent of } x \\ \text{(Output / Label)} \quad &y = x^\top w_0 + \epsilon. \end{aligned} \right\} \quad (2)$$

The positive integer d is the input-dimension, the vector $w_0 \in \mathbb{R}^d$ defines the ground-truth labelling function $x \mapsto x^\top w_0$, the matrix $\Sigma \in \mathbb{R}^{d \times d}$ is the covariance structure of the inputs. The scalar σ^2 is the level of label noise. To begin, we consider the linear case for clarity. We shall discuss the kernel setting at the end of this section. Thus, in classical linear regression, we are given a sample $(X, Y) \equiv \{(x_1, y_1), \dots, (x_T, y_T)\}$ of size T from $P_{\Sigma, w_0, \sigma^2}$ and we

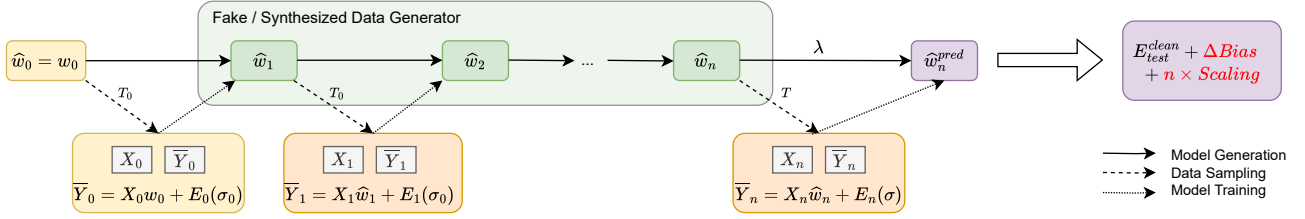


Figure 4. Illustration of the theoretical framework. The process begins with the original model $\hat{w}_0(w_0)$ and the original dataset (X_0, \bar{Y}_0) . n synthetic data generators \hat{w}_1 to \hat{w}_n are iteratively fit on data labelled by the previous model with label noise σ_0 , using T_0 samples each. We evaluate the test error of \hat{w}_n^{pred} (with respect to the ground truth labels from w_0), which is trained on $(X, Y) := (X_n, \bar{Y}_n)$ using T samples and a regularization coefficient λ .

seek a linear model $\hat{w} \in \mathbb{R}^d$ with small test error

$$\begin{aligned} E_{test}(\hat{w}) &:= \mathbb{E}_{\bar{w}} \mathbb{E}_{x,y} [(x^\top \hat{w} - y)^2] - \sigma^2 \\ &= \mathbb{E}_{\bar{w}} [\|\hat{w} - w_0\|_{\Sigma}^2], \end{aligned} \quad (3)$$

where $(x, y) \sim P_{\Sigma, w_0, \sigma^2}$ is a random clean test point.

In our setup for studying model collapse, the training data (X, Y) is sampled from an iterative loop where each generation of the model serves as the labeller for the data for the next generation. This process is described below.

Construction of Fake / Synthesized Data Generator.

$$P_{\Sigma, w_0, \sigma_0^2} \rightarrow P_{\Sigma, \hat{w}_1, \sigma_1^2} \rightarrow \dots \rightarrow P_{\Sigma, \hat{w}_n, \sigma_n^2} \rightarrow \dots, \quad (4)$$

where the sequence of models $(\hat{w}_n)_{n \in \mathbb{N}}$ is defined recursively by

$$\hat{w}_n = \begin{cases} w_0, & \text{if } n = 0, \\ \text{Fit}(X_{n-1}, \bar{Y}_{n-1}), & \text{if } n \geq 1, \end{cases} \quad (5)$$

where $\bar{Y}_n := X_n \hat{w}_n + E_n$ and $\text{Fit}(A, B) = \text{OLS}(A, B) := A^\dagger B$ is ordinary-least squares (OLS).

The design matrices $(X_n)_{n \geq 0}$ are of shapes $T_n \times d$, each with iid rows from $N(0, \Sigma)$.

The sequence of noise vectors $(E_n)_{n \geq 0}$ forms an independent collection, which is independent of the $(X_n)_{n \geq 0}$; each $E_n = (\epsilon_{n,1}, \dots, \epsilon_{n,T_n})$ has length T_n and iid components from $N(0, \sigma_n^2)$. This is summarized in Figure 4.

Thus, in summary, each \hat{w}_n results from fitting a model on a dataset of size T_{n-1} from $P_{\Sigma, \hat{w}_{n-1}, \sigma_{n-1}^2}$, for every $n \geq 1$. Importantly, the downstream model (introduced later) has no control over this process. It will only see training data from a given version $P_{\Sigma, \hat{w}_n, \sigma_n^2}$, but will be tested on the true distribution $P_{\Sigma, w_0, \sigma_0^2}$.

The Downstream Model: Ridge Regression. For a number of iterations $n \geq 0$, noise levels σ_0 and σ , dataset sizes T_0 and T , and regularization parameter $\lambda \geq 0$, let $\hat{w}_n^{pred} =$

$\hat{w}_{n, T_0, \sigma_0^2, T, \sigma, \lambda}^{pred} \in \mathbb{R}^d$ be the ridge predictor constructed from an iid sample $\{(x_1, y_1), \dots, (x_T, y_T)\}$ of size T from the n -fold fake data distribution $P_{\Sigma, \hat{w}_n, \sigma_n^2}$, where for ease of presentation of our results we will assume that

$$\left. \begin{aligned} T_{n-1} &= \dots = T_1 = T_0, & T_n &= T \\ \sigma_{n-1} &= \dots = \sigma_1 = \sigma_0, & \sigma_n &= \sigma. \end{aligned} \right\} \quad (6)$$

Downstream Ridge Predictor.

For an n -fold fake data generator $P_{\Sigma, \hat{w}_n, \sigma_n^2}$, we denote with $X := X_n \in \mathbb{R}^{T \times d}$ the design matrix with iid rows from $N(0, \Sigma)$, with $E := E_n \in \mathbb{R}^T$ the error vector with components in $N(0, \sigma_n^2)$, and $Y := \bar{Y}_n = X \hat{w}_n + E \in \mathbb{R}^T$ the labels generated by $P_{\Sigma, \hat{w}_n, \sigma_n^2}$. Then

$$\hat{w}_n^{pred} = \begin{cases} X^\dagger Y, & \text{if } \lambda = 0, \\ R X^\top Y / T, & \text{otherwise,} \end{cases} \quad (7)$$

where

$$\hat{\Sigma} := X^\top X / T \in \mathbb{R}^{d \times d}$$

is the sample covariance matrix, and

$$R = R(\lambda) := (\hat{\Sigma} + \lambda I_d)^{-1}$$

denotes its resolvent.

We are interested in the dynamics of the test error $E_{test}(\hat{w}_n^{pred})$ (according to formula (3)) of this linear model. Importantly, the evaluation of the model is performed on the true data distribution $P_{\Sigma, w_0, \sigma_0^2}$, even though the model is trained on the fake data distribution $P_{\Sigma, \hat{w}_n, \sigma_n^2}$. Note that for $n = 0$, $E_{test}^{clean} := E_{test}(\hat{w}_n^{pred})$ corresponds to the usual test error when the downstream model is trained on clean data.

The mental picture is as follows: each generation \hat{w}_n can be seen as a proxy for a specific version of ChatGPT, for example. The sample size T_0 used to create the fake labelling functions \hat{w}_n is a proxy for the strength of the fake

data-generator thus constructed. Other works which have considered model collapse under such a self-looping training process include Shumailov et al. (2023); Alemohammad et al. (2023); Bertrand et al. (2023); Dohmatob et al. (2024).

A Note on Extension to Kernel Methods Though we present our results in the case of linear regression in \mathbb{R}^d for clarity, they can be rewritten in equivalent form in the kernel setting. Indeed, as in Caponnetto & de Vito (2007); Simon et al. (2021); Cui et al. (2022); Liang & Rakhlin (2020), it suffices to replace x with a feature map induced by a kernel K , namely $\psi(x) := K_x \in \mathcal{H}_K$. Here, \mathcal{H}_K is the reproducing kernel Hilbert space (RKHS) induced by K . In the data distribution (2), we must now replace the Gaussian marginal distribution condition $x \sim N(0, \Sigma)$ with $\psi(x) \sim N(0, \Sigma)$. The ground-truth labeling linear function in (2) is now just a general function $f_0 \in L^2$. The ridge predictor (7) is then given by (*Representer Theorem*) $\hat{f}_n^{\text{pred}}(x) := K(X, x)^\top \hat{c}_n$, with $\hat{c}_n = (G + \lambda \Gamma I_d)^{-1} Y \in \mathbb{R}^n$, where $K(X) := (K_{x_1}, \dots, K_{x_T})$, and $G = K(X)K(X)^\top = K(X, X) = (K(x_i, x_j))_{1 \leq i, j \leq T} \in \mathbb{R}^{n \times n}$ is the Gram matrix.

4. Exact Test Error Characterization

In this section we establish generic analytic formulae for the test error of the downstream model \hat{w}_n^{pred} (7) trained on n -fold fake data-generation as outlined in Section 3. All proofs of this section are relegated to Appendix A.

4.1. Warm-up: Unregularized Case

For a start, let us first consider the case of ridgeless regression (corresponding to $\lambda = 0$ in Equation (7)), which amounts to OLS.

Theorem 4.1. *For an n -fold fake data generation process with $T_0 \geq d + 2$ samples, the test error for the linear predictor \hat{w}_n^{pred} given in (7) learned on $T \geq d + 2$ samples, with $\lambda = 0$ (i.e. unregularized), is given by*

$$E_{\text{test}}(\hat{w}_n^{\text{pred}}) \simeq \frac{\sigma^2 \phi}{1 - \phi} + \frac{n \sigma_0^2 \phi_0}{1 - \phi_0}, \quad (8)$$

with $\phi = \frac{d}{T}$, $\phi_0 = \frac{d}{T_0}$.

The first term $E_{\text{test}}(\hat{w}_0^{\text{pred}}) \simeq \sigma^2 \phi / (1 - \phi)$ corresponds to the usual error when the downstream model is fitted on clean data (see Hastie et al. (2022), for example). The additional term $n \sigma_0^2 \phi_0 / (1 - \phi_0)$, proportional to the number of generations n , is responsible for model collapse.

Remark 4.2. *Note that the linear degeneration in test error highlighted by Equation (8) is a direct consequence of using the same dataset size T_0 across the fake data generator. Of course, if the underlying synthetic generating process has access to a larger data budget across generations, this*

decay can be significantly alleviated. For instance, if fake data increases gradually with the number of generations m as $T_m = mT$ (and, to simplify, $\sigma = \sigma_0$) a trivial extension of Theorem 4.1 yields

$$E_{\text{test}}(\hat{w}_n^{\text{pred}}) \simeq (1 + \frac{1}{2} + \frac{1}{3} + \dots) E_{\text{test}}(\hat{w}_0^{\text{pred}}) \\ \simeq \log n \cdot E_{\text{test}}(\hat{w}_0^{\text{pred}}),$$

which will keep collapse at bay at the expense of largely increased training data. This does not avoid model collapse; rather, it trades additional data generation and training effort against deterioration from generations of fake data. Thus, while for clean data increasing the dataset size n -fold leads to better scaling, with synthetic data, we not only forfeit this improvement but also experience a degeneration. Also, note that we do not assume access to samples from any of the intermediate generation steps $\hat{w}_0, \dots, \hat{w}_{n-1}$; we only train the downstream model \hat{w}_n^{pred} on data from the last step \hat{w}_n . Using intermediate data could in principle, allow to effectively escape collapse, of course, again, at increased data budget.

Low-Dimensional Regime. In the low-dimensional regime (fixed d), Theorem 4.1 already predicts a change of scaling law from $E_{\text{test}}(\hat{w}_0^{\text{pred}}) \asymp \sigma^2 T^{-1}$ to $E_{\text{test}}(\hat{w}_n^{\text{pred}}) \asymp \sigma^2 T^{-1} + n \sigma_0^2 T_0^{-1}$. Thus, as the sample size T is scaled up, the test error eventually plateaus at the value $n \sigma_0^2 T_0^{-1}$ and does not vanish. This phenomenon is clearly visible in Figure 1. In Section 5, we shall establish an analogous picture for high-dimensional regimes ($d \rightarrow \infty$).

Mitigation via Regularization ? Note that the test error of the null predictor $w_{\text{null}} = 0$ is $E_{\text{test}}(w_{\text{null}}) = \|w_0\|_\Sigma^2$, and so

$$\frac{E_{\text{test}}(\hat{w}_n^{\text{pred}})}{E_{\text{test}}(w_{\text{null}})} = \frac{1}{\text{SNR}} \frac{\phi}{1 - \phi} + \frac{n}{\text{SNR}_0} \frac{\phi_0}{1 - \phi_0},$$

where $\text{SNR} := \|w_0\|_\Sigma^2 / \sigma^2$ and $\text{SNR}_0 := \|w_0\|_\Sigma^2 / \sigma_0^2$. We deduce that if $n \gg \text{SNR}_0 / (1/\phi_0 - 1)$, then the learned model is already much worse than the null predictor! This suggests that a good strategy for mitigating the negative effects on learning on AI-generated data is regularization at an appropriate level, as illustrated in Figure 5.

4.2. Main Result I: A General Formula for Test Error

We now consider the case of general ridge penalty $\lambda > 0$, and drop the requirements $T \geq d + 2$ and $T_0 \geq d + 2$.

Recall the definitions of X, Y, E and the random matrices R and $\hat{\Sigma}$ appearing in (7). For later reference, define

$$\text{Bias} := \mathbb{E} \|\hat{\Sigma} R w_0 - w_0\|_\Sigma^2, \quad (9)$$

$$\text{Var} = \mathbb{E} \|R X^\top E / T\|_\Sigma^2 = \sigma^2 \frac{1}{T} \text{tr} \Sigma R^2 \hat{\Sigma}. \quad (10)$$

These are respectively the bias and variance terms in the classical bias-variance decomposition of the test error

$$E_{test}^{clean} := Bias + Var, \quad (11)$$

for standard ridge regression fitted on clean data from the true data distribution $P_{\Sigma, w_0, \sigma^2}$ (e.g., see Hastie et al. (2022)).

Theorem 4.3. *For an n -fold fake data generation process, the test error of a ridge predictor \hat{w}_n^{pred} based on a sample of size $T \geq 1$ with regularization parameter λ is given by*

$$\left. \begin{aligned} E_{test}(\hat{w}_n^{pred}) &= \widetilde{Bias} + Var + n\sigma_0^2\rho, \\ \widetilde{Bias} &= \mathbb{E} \|\widehat{\Sigma} R Q_{n-1} w_0 - w_0\|_{\Sigma}^2, \\ \rho &:= \frac{1}{n} \sum_{m=0}^{n-1} \mathbb{E} \operatorname{tr} C_{n-1, m} \widehat{\Sigma} R \Sigma R \widehat{\Sigma}, \end{aligned} \right\} \quad (12)$$

where Var is as given in (10) and $C_{k, m} := \overline{Q}_{k, m} \overline{Q}_{k, m}^\top$ for $\overline{Q}_{k, m} = Q_{k, m} X_m^\dagger$, $Q_{k, m} := P_k P_{k-1} \dots P_m$, $Q_k := Q_{k, 0} = P_k P_{k-1} \dots P_0$, with $P_m = X_m^\dagger X_m$ being the orthogonal projection matrix onto the subspace of \mathbb{R}^d spanned by the rows of X_m .

In particular, if $T_0 \geq d + 2$ (under-parametrized data-generator), then $\widetilde{Bias} = Bias$ as given in (9), and

$$\left. \begin{aligned} E_{test}(\hat{w}_n^{pred}) &\simeq E_{test}^{clean} + n\sigma_0^2\rho, \\ \rho &= \frac{1}{T_0 - d - 1} \mathbb{E} \operatorname{tr} \Sigma^{-1} \widehat{\Sigma} R \Sigma \widehat{\Sigma} R. \end{aligned} \right\} \quad (13)$$

In the second part of the theorem, the term E_{test}^{clean} (introduced earlier in (11)) corresponds to the usual test error when the downstream model is trained on real (not fake) data, for which well-known formulae exist in a variety of scenarios (see Proposition 4.5).

Remark 4.4. *We shall later show in Theorem 4.6 that $\widetilde{Bias} \geq Bias + \Delta Bias$, where $\Delta Bias \geq 0$ in the appropriate asymptotic limit, with equality if $T_0 \geq d + 2$ (the under-parametrized regime). Thus, apart from the variance term, an over-parametrized ($T_0 < d + 2$) synthetic data-generator harms the bias term of the test error of downstream models. In contrast, an under-parametrized synthetic data-generator ($T_0 \geq d + 2$) only harms the variance. The increase in bias suffered in the over-parametrized regime will be precisely quantified in Section 4.6, and shown to be an increasing function of the number of generations n .*

The test error decomposition in Theorem 4.3 is thus of the promised form (1), with $Scaling = \sigma_0^2\rho$. This additional term means that there is competition between the usual test error E_{test}^{clean} and the additional term induced by the fake labeling process. Understanding the interaction of these two terms is key to demystifying the origins of model collapse.

Low-Dimensional Limit. Observe that if d is fixed and $T \rightarrow \infty$, then the empirical covariance matrix $\widehat{\Sigma}$ converges to¹ its population version Σ , and so for $T_0 \geq d + 2$, we have

$$\rho \simeq \frac{\operatorname{tr} \Sigma^2 (\Sigma + \lambda I_d)^{-2}}{T_0 - d} = \frac{df_2(\lambda)}{T_0 - d},$$

where for any $\lambda \geq 0$ and $m \in \mathbb{N}_*$, $df_m(\lambda)$ is the m th order "degree of freedom" of the covariance matrix Σ is given by

$$df_m(\lambda) = df_m(\lambda; \Sigma) := \operatorname{tr} \Sigma^m (\Sigma + \lambda I_d)^{-m}.$$

Note that $df_m(\lambda) \leq d$ always. In the high-dimensional setting (where d can grow beyond T_0), the precise analysis of ρ will be carried out via random matrix theory (RMT).

4.3. High-Dimensional Regimes in the RMT limit

In order to analyze the trace term ρ appearing in (12), we need some tools from RMT, and ultimately obtain analytic formulae for $E_{test}(\hat{w}_n^{pred})$ in Theorem 4.6. Such tools have been used extensively to analyze anisotropic ridge regression Richards et al. (2021); Hastie et al. (2022); Bach (2023). A standard reference on RMT is Bai & Silverstein (2010).

Random Matrix Equivalents. For any sample size $T \geq 1$, define an increasing function $\lambda \rightarrow \kappa(\lambda, T)$ implicitly by

$$\kappa(\lambda, T) - \lambda = \kappa(\lambda, T) \cdot df_1(\kappa(\lambda, T))/T. \quad (14)$$

The effect of ridge regularization at level $\lambda \geq 0$ is to improve the condition of the empirical covariance matrix $\widehat{\Sigma}$; what the κ -function does is translate this into regularization on Σ at level $\kappa(\lambda, T)$, so as control the capacity of the former, i.e. the "effective dimension" of the underlying problem. Quantitatively, there is an equivalence of the form

$$df_1(\lambda; \widehat{\Sigma}) \approx df_1(\kappa(\lambda, T); \Sigma).$$

Roughly speaking, RMT is the business of formalizing such a relationship and derivatives (w.r.t. λ) thereof.

Example: Isotropic Covariance. As an illustration, note that $df_m(\lambda) \equiv d/(1 + \lambda)^m$ (polynomial decay) in the isotropic case where $\Sigma = I_d$. Consequently, we have

$$\kappa(\lambda, T) - \lambda = \phi \cdot \kappa(\lambda, T)/(1 + \kappa(\lambda, T)), \quad \text{with } \phi := d/T.$$

In this case, it is easy to obtain the following well-known formula for $\kappa = \kappa(\lambda, T)$:

$$\kappa = \frac{1}{2} \left(\lambda + \bar{\phi} + \sqrt{(\lambda + \bar{\phi})^2 + 4\lambda} \right), \quad \text{with } \bar{\phi} := \phi - 1, \quad (15)$$

which is reminiscent of the celebrated Marchenko-Pastur law (Marčenko & Pastur, 1967).

¹e.g. weakly, w.r.t. operator-norm.

Furthermore, we shall work in the following so-called proportionate asymptotic scaling which is a standard analysis based on random matrix theory (RMT):

$$T, d \rightarrow \infty, d/T \rightarrow \phi, \|\Sigma\|_{op}, \|\Sigma^{-1}\|_{op} = O(1). \quad (16)$$

Later in Section 5 when we consider power-law spectra, this scaling will be extended to account for the more realistic case where d and T are of the same order on log scale, i.e

$$T, d \rightarrow \infty, d^{1/C} \lesssim T \lesssim d^C, \|\Sigma\|_{op}, \|\Sigma^{-1}\|_{op} = O(1), \quad (17)$$

for some absolute constant $C \geq 1$. Such non-proportionate settings are covered by the theory developed in Knowles & Yin (2017); Wei et al. (2022). For clarity of presentation, even in this more general regime (17), we will still continue to write $\phi_0 := d/T_0$ and $\phi := d/T$.

Bias-Variance Decomposition. With everything now in place, let us recall for later use, the following classical bias-variance decomposition for ridge regression (for example, see Richards et al. (2021); Hastie et al. (2022); Bach (2023)):

Proposition 4.5. *In the RMT limit (17), the test error of a ridge predictor $w(\lambda)$ based on T iid samples from the true data distribution $P_{\Sigma, w_0, \sigma^2}$ is given by*

$$E_{test}(w(\lambda)) = \mathbb{E} \|w(\lambda) - w_0\|_{\Sigma}^2 \simeq Bias + Var, \quad (18)$$

$$Bias \simeq \frac{\kappa^2 w_0^\top \Sigma (\Sigma + \kappa I)^{-2} w_0}{1 - df_2(\kappa)/T},$$

$$Var \simeq \frac{\sigma^2 df_2(\kappa)}{T} \cdot \frac{1}{1 - df_2(\kappa)/T}, \quad (19)$$

where $\kappa = \kappa(\lambda, T)$ is as given in (14).

In particular, in the isotropic case where $\Sigma = I_d$, we have

$$E_{test}(w(\lambda)) \simeq \frac{\kappa^2 \|w_0\|_2^2 + \sigma^2 \phi}{(1 + \kappa)^2 - \phi},$$

where $\phi := d/T$ and $\kappa = \kappa(\lambda, T)$ is as given in (15).

4.4. Main Result II: Analytic Formula for Test Error

The following result gives the test error for the downstream ridge predictor \hat{w}_n^{pred} defined in (7), in the context of fake training data, and will be heavily exploited later to obtain precise estimates in different regimes. For later reference, define $\Delta Bias \geq 0$ by

$$\Delta Bias := \mathbb{E} \|\hat{\Sigma} R(Q_{n-1} w_0 - w_0)\|_{\Sigma}^2, \quad (20)$$

where the matrix Q_{n-1} is as defined in Theorem 4.3.

Theorem 4.6. *For an n -fold fake data-generation process, the test error of a ridge predictor \hat{w}_n^{pred} based on a sample of size T with regularization parameter λ , is given in the RMT limit (17) by*

$$E_{test}(\hat{w}_n^{pred}) \simeq \widetilde{Bias} + Var + n\sigma_0^2 \rho, \quad (21)$$

where Var and ρ are as given in Theorem 4.3, and \widetilde{Bias} satisfies

$$\widetilde{Bias} \geq Bias + \Delta Bias \geq Bias \quad (\text{with equality if } T_0 \geq d),$$

and $\Delta Bias$ as given in 20.

Furthermore, if one of the following conditions holds

$$T_0 \geq d \text{ OR } X_n = X_0 \text{ for all } n, \quad (22)$$

then, we have the following explicit formula for ρ

$$\rho = \frac{\text{tr} \Sigma^4 (\Sigma + \kappa_0 I)^{-2} (\Sigma + \kappa I)^{-2}}{T_0 - df_2(\kappa_0)} + \frac{\kappa^2 \text{tr} \Sigma^2 (\Sigma + \kappa_0 I)^{-2} (\Sigma + \kappa I)^{-2}}{T_0 - df_2(\kappa_0)} \cdot \frac{df_2(\kappa)}{T - df_2(\kappa)},$$

with $\kappa = \kappa(\lambda, T)$ and $\kappa_0 := \kappa(0, T_0)$ are as given in (14).

Instructively, the term $\Delta Bias$ measures how biased the synthetic data-generation process away from ground-truth model w_0 . This term disappears if the generator was fitted on sufficiently many samples (i.e. if $T_0 \geq d$). More quantitatively, when $T_0 < d$ and $X_n = X_0$, it is easy to see that $\Delta Bias \geq \mathbb{E} [\|\Sigma^{1/2} \hat{\Sigma} R\|_{op}^2] \cdot Bias_0$, where $Bias_0 := \mathbb{E} \|P_0 w_0 - w_0\|_2^2$ measures the inability due to lack of enough data, of the first generation ($n = 1$) to reliably estimate w_0 even in the absence of noise ($\sigma_0 = 0$) in the data-generating process. This gap propagates over to higher generations of the process. The situation is illustrated in Figure 3. In the case where $T_0 < d$ and the X_n 's are independent, we shall see in Section 4.6 that this increase in bias actually grows with n , even when $\sigma_0 = 0$.

4.5. Under-Parametrized Fake Data-Generator

Observe that if $T_0 \geq d$, then $P_0 = I_d$ a.s., leading to $\widetilde{Bias} = Bias$ (given as in formula (18)), and $\kappa_0 = 0$ in Theorem 4.3, and

$$\rho = \frac{df_2(\kappa)}{T_0 - d} + \frac{\kappa^2 \text{tr} (\Sigma + \kappa I)^{-2}}{T_0 - d} \frac{df_2(\kappa)}{T - df_2(\kappa)}, \quad (23)$$

with κ as in Theorem 4.3. We have the following corollary.

Corollary 4.7. *Consider the setting of Theorem 4.3. If $T_0 \geq d$ additionally, then it holds in the RMT limit (17) that*

$$E_{test}(\hat{w}_n^{pred}) \simeq Bias + Var + n\sigma_0^2 \rho,$$

where $Bias$ and Var are as given in formulae (18) and (19) respectively, and ρ is as given in (23).

In the special case of isotropic features, it holds that

$$Bias + Var \simeq \frac{\kappa^2 \|w_0\|_2^2 + \sigma^2 \phi}{(1 + \kappa)^2 - \phi},$$

$$\rho \simeq \frac{\phi_0}{1 - \phi_0} \left(\frac{1}{(1 + \kappa)^2} + \frac{1}{(1 + \kappa)^2} \frac{\phi \kappa^2}{(1 + \kappa)^2 - \phi} \right),$$

with $\phi := d/T$, $\phi_0 := d/T_0$, and $\kappa = \kappa(\lambda, T)$ as in (15).

Such a result gives us the needed analytical handle for understanding n -fold model collapse in terms of all problem hyper-parameters (covariance spectrum, regularization, label-noise level, etc.).

4.6. Model Collapse in the Absence of Label Noise

We now consider the over-parametrized regime, where the different iterations of the synthetic data-generator (refer to the illustration in Figure 4) are fitted on insufficient data. For simplicity of exposition, we restrict our presentation to isotropic covariance $\Sigma = I_d$. Since we will be focusing on the possible increase $\Delta Bias$ in bias (defined in (18)) due to $n \geq 1$ generations as predicted by Theorem 4.6, we further restrict ourselves to the noiseless regime where the fake data-generating process has no label noise, i.e $\sigma_0 = 0$. Thanks to Lemma A.2, we know that the generation- n fake labelling vector \hat{w}_n is in this setting given explicitly by the formula

$$\hat{w}_n = P_{n-1}P_{n-2} \dots P_0 w_0, \quad (24)$$

where, as usual, $P_m \in \mathbb{R}^{d \times d}$ is the orthogonal projection matrix onto the subspace of \mathbb{R}^d spanned by the rows of X_m . Further, for simplicity we will assume $T = T_n > d$, i.e the downstream model has access to enough data.

We shall focus on two important special cases.

Dependent Case. We first consider the case where $T_m = T_0 < d$ and $X_m = X_0$ for all $m \leq n - 1$. It is clear that (24) reduces to $\hat{w}_n = P_0 w_0$. We have the following result.

Theorem 4.8. *In the limit $\lambda \rightarrow 0^+$ and $d, T_0 \rightarrow \infty$ with $d/T_0 \rightarrow \phi_0 > 1$, it holds that*

$$\|\hat{w}_n\|^2 \simeq \|w_0\|^2 / \phi_0, \quad (25)$$

$$\Delta Bias \simeq \|w_0\|^2 (1 - 1/\phi_0). \quad (26)$$

We see that in this setting, the increase in bias $\Delta Bias \simeq (1 - 1/\phi_0)\|w_0\|^2$ brought about by synthetic data is a positive constant which does not grow with the number of generations $n \geq 1$. This increase in bias (i.e compared to training on clean data) is due to the fact that, with probability 1, the random subspace of \mathbb{R}^d spanned by X_0 does not contain the ground truth model w_0 . The expression is nothing but a RMT estimate of $\|P_0 w_0 - w_0\|^2$, i.e the squared norm of the projection of w_0 onto the orthogonal complement of this subspace. The result is illustrated in Figure 3(a).

Independent Case. For our second example, we remove the assumption that $T_m = T_0$ and $X_m = X_0$ for all $m \leq n - 1$ considered in the previous case (Theorem 4.8). We instead assume that

- the X_m 's are assumed to be independent, and
- we are in the following high-dimensional limit

$$d, T_1, \dots, T_{n-1} \rightarrow \infty, \quad d/T_m \rightarrow \phi_m, \quad (27)$$

where $\phi_1, \dots, \phi_{n-1}$ are positive constants.

We have the following theorem.

Theorem 4.9. *In the limit (27) and $\lambda \rightarrow 0^+$, it holds that*

$$\|\hat{w}_n\|^2 \simeq \|w_0\|^2 \prod_{m=0}^{n-1} \min(1/\phi_m, 1), \quad (28)$$

$$\Delta Bias \simeq \|w_0\|^2 \left(1 - \prod_{m=0}^{n-1} \min(1/\phi_m, 1) \right). \quad (29)$$

In particular, if $n \rightarrow \infty$ such that infinitely many of the ϕ_m 's are > 1 , then $\hat{w}_n \rightarrow 0$ and $\Delta Bias \rightarrow \|w_0\|^2$.

The theorem predicts that a sequence of over-parametrized fake data-generators $(\hat{w}_n)_n$ collapses to zero (and thus, effectively escapes from the ground truth model w_0). Consequently, the downstream model \hat{w}_n^{pred} converges to a Gaussian process around zero, instead of the true model w_0 , leading to an increase in the bias term of the test error!

For example if $\phi_m = \phi_0 > 1$ for all $m \leq n - 1$, then

$$\Delta Bias \simeq (1 - \phi_0^{-n})\|w_0\|^2,$$

which grows exponentially fast towards $\|w_0\|^2$, the test error of the null predictor. This compounding effect is due to the fact that in (24), each projection P_m spins the fake data labelling vector \hat{w}_n away from the ground-truth w_0 even further. The result is illustrated in Figure 3(b).

5. The Case of Heavy Tails (Power Law)

Now, consider a variant of the distribution (2), in the setting considered in Caponnetto & de Vito (2007); Richards et al. (2021); Simon et al. (2021); Cui et al. (2022), for $d \rightarrow \infty$. Let the spectral decomposition of Σ be

$$\Sigma = \lambda_1 v_1 v_1^\top + \dots + \lambda_d v_d v_d^\top,$$

where $\lambda_1 \geq \dots \geq \lambda_d \geq 0$ are the eigenvalues and $v_1, \dots, v_d \in \mathbb{R}^d$ are the eigenvectors. For any j , define a coefficient $c_j := w_0^\top v_j$, i.e the projection of w_0 along the j th eigenvector of Σ .

We shall work under the following spectral conditions

$$\left. \begin{array}{l} \text{(Capacity Condition)} \lambda_j \asymp j^{-\beta} \text{ for all } j \in [d], \\ \text{(Source Condition)} \|\Sigma^{1/2-r} w_0\| = O(1), \end{array} \right\} \quad (30)$$

where $\beta > 1$ and $r \geq 0$. The parameter r measures the amount of dispersion of w_0 relative to the spectrum of Σ ;

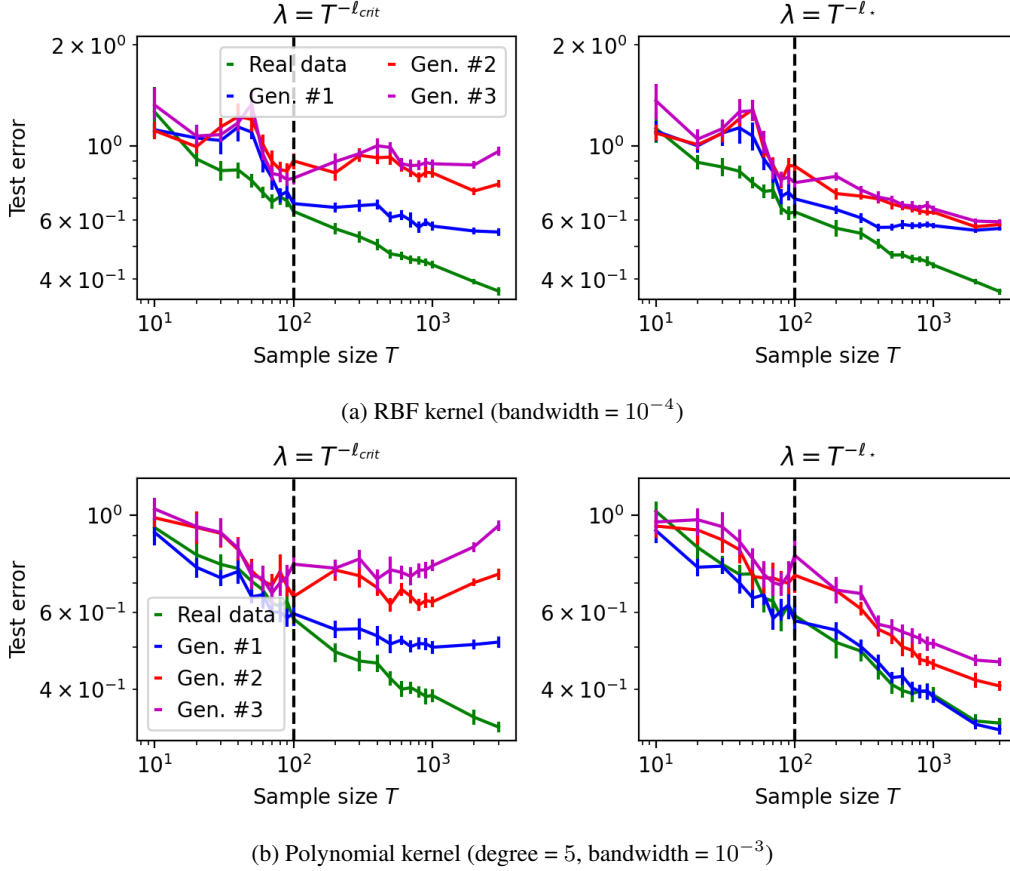


Figure 5. Demystifying model collapse in kernel ridge regression (power-law covariance spectrum) on MNIST. Here, we use adaptive regularization $T^{-\ell}$ for different values of the exponent $\ell \geq 0$ (see Section 6 for full experimental setup). **Top row:** RBF kernel. **Bottom row:** polynomial kernel. In each plot, we show test error curves as a function of sample size T , from different generations (n) of fake data. The broken vertical line corresponds to $T = T_0$, where T_0 is the number of samples (from the true data distribution) which was used to train the label faker. The value of the exponent regularization $\ell = \ell_*$ (broken curves) is the optimal value in the presence of iterative data relabeling, while $\ell = \ell_{crit}$ (solid curves) corresponds to the optimal value without iterative re-labelling (i.e. $n = 0$) proposed in Cui et al. (2022) (see (32)). Specifically, we take $\ell_* = (b - a)\ell_{crit} = b\ell_{crit}$, where $b = \log T_0 / \log T$ (so that $T_0 = T^b$), as proposed in Theorem 5.2, formula (33). Notice how the effect of fake data makes the test error become non decreasing in sample size T . This is effectively a collapse of the learned model.

a large value of r means w_0 is concentrated only along a few important eigen-directions (i.e. the learning problem is easy). For later convenience, define \underline{r} and δ by

$$\underline{r} := \min(r, 1), \quad \delta := 1 + \beta(2r - 1).$$

As noted in Cui et al. (2022), the source condition in (30) is satisfied if $c_j \asymp j^{-\delta/2}$ for all $j \in [d]$.

Consider adaptive ridge regularization strength of the form

$$\lambda = \lambda(T) \asymp T^{-\ell}, \quad (31)$$

for fixed $\ell \geq 0$. The case where $\ell = 0$ corresponds to non-adaptive regularization; otherwise, the level of regularization decays polynomially with the sample size T . Define

$$\ell_{crit} := \beta / (1 + 2\beta\underline{r}). \quad (32)$$

In Cui et al. (2022) KRR under normal circumstances (corresponding to $n = 0$, i.e. no fake data) was considered and it was shown that this value for the regularization exponent in (31) is minimax-optimal for normal test error in the noisy regime ($\sigma > 0$), namely $E_{test}(\hat{w}_0^{pred}) \asymp T^{-c}$, where

$$c := \frac{2\beta\underline{r}}{2\beta\underline{r} + 1} \in (0, 1).$$

This represents a crossover from the noiseless regime where it was shown that the test error scales like $E_{test}(\hat{w}_0^{pred}) \asymp T^{-2\beta\underline{r}}$, a much faster rate. We shall show that the picture drastically changes in the context of training on fake data considered in this manuscript for the purpose of understanding model collapse (Shumailov et al., 2023).

Remark 5.1. Unlike Cui et al. (2022) which considered the proportionate scaling limit (16) for input dimension d and sample size T , we shall consider the more general (and

more realistic) polynomial scaling limit (17), and invoke the tools of so-called anisotropic local RMT developed in Knowles & Yin (2017) to compute deterministic equivalents for quantities involving the spectra of random matrices.

5.1. Main Result III: A "Collapsed" Scaling Law

The following result shows that model collapse is a modification of usual scaling laws induced by fake data. All proofs of this section can be found in Appendix B. Here, we restrict to the case $T_0 \geq d + 2$ to make the results easier to present. This condition can be removed as in Theorem 4.6.

Theorem 5.2. *Consider n -fold fake-data generation with sample size $T_0 \geq d + 2$. For a ridge predictor \hat{w}_n^{pred} given in (7) based on a fake data sample of size T , with regularization parameter $\lambda = \lambda(T)$ tuned adaptively as in (31) with exponent $\ell \in [0, \beta)$, the test error satisfies the following scaling law in the RMT limit (17):*

$$E_{\text{test}}(\hat{w}_n^{\text{pred}}) \asymp \max(\sigma^2, T^{1-2r\ell-\ell/\beta}) \cdot T^{-(1-\ell/\beta)} + \frac{n\sigma_0^2}{1-\phi_0} \max(T/T_0, \phi_0) \cdot T^{-(1-\ell/\beta)}.$$

5.2. Optimal Regularization for Mitigating Collapse

Let us provide an instructive interpretation of the result.

Noiseless Regime. Suppose $\sigma = 0$ (or equivalently, exponentially small in T) and $\phi_0 \in (0, 1)$ is fixed, and consider a number of generations n such that $n\sigma_0^2 \asymp T^a$, where $0 \leq a \leq 1 - \ell/\beta \leq 1$. Note that $a = 0$ corresponds to a constant number of generations. Also take $T_0 = T^b$, for some constant $b \in (0, \infty)$. According to Theorem 5.2, if we want to balance out the model-collapsing negative effect of training on fake data, we should chose ℓ so as to balance the second term $n(T/T_0)T^{-(1-\ell/\beta)} = T^{-(b-\ell/\beta-a)}$ and the first term $T^{-2\ell r}$. This gives the following result.

Corollary 5.3. *In the setting of Theorem 5.2 with $T_0 \asymp T^b$ and $n \asymp T^b$, the optimal exponent of the ridge regularization parameter in (31) is $\ell = \ell_*$, where*

$$\ell_* = \min((b-a)\ell_{\text{crit}}, \beta), \quad (33)$$

and ℓ_{crit} is as in (32), with corresponding optimal test error

$$\inf_{\ell \geq 0} E_{\text{test}}(\hat{w}_n^{\text{pred}}) \asymp E_{\text{test}}(\hat{w}_n^{\text{pred}})|_{\ell=\ell_*} \asymp T^{-(b-a)c}.$$

Observe that when $(b-a)c < 2\beta r$, which is the case when $n = O(1)$, $r \geq 1$ and $b \leq a + 1$, this corresponds to the condition $T \gtrsim T_0$. The above result represents a crossover from the fast rate $E_{\text{test}}(\hat{w}_0^{\text{pred}}) \asymp T^{-2\beta r}$ in the case of training on clean data Cui et al. (2022), to a much slower rate $E_{\text{test}}(\hat{w}_n^{\text{pred}}) \asymp T^{-(b-a)c}$, attained by the adaptive regularization $\lambda \asymp T^{-\ell_*}$, which is optimal in this setting.

Furthermore, in this setting if we still use $\lambda \asymp T^{-\ell_{\text{crit}}}$ as proposed in Cui et al. (2022) in the clean data setting, Corollary 5.3 predicts that

$$E_{\text{test}}(\hat{w}_n^{\text{pred}}) \gtrsim T^{-(b-\ell_{\text{crit}}/\beta-a)} = T^{-(c+b-a-1)},$$

which diverges to infinity if $b \geq a + 1 - c$. This is a catastrophic form of model collapse, and is empirically illustrated in Figures 2 and 5.

Noisy Regime. Now fix $\sigma^2 \neq 0$ and $\phi_0 \in (0, 1)$. In this regime, Theorem 5.2 predicts that consistency (i.e. $E_{\text{test}}(\hat{w}_n^{\text{pred}}) \xrightarrow{T \rightarrow \infty} 0$) is only possible if $\ell \leq \ell_*$. First consider values of ℓ for which the clean variance $\sigma^2 T^{-(1-\ell/\beta)}$ is smaller than the clean bias $T^{-2r\ell}$ in (33) i.e. $0 \leq \ell \leq \ell_{\text{crit}}$. We get

$$E_{\text{test}}(\hat{w}_n^{\text{pred}}) \asymp T^{-2r\ell} + T^{-(b-a-\ell/\beta)},$$

which is minimized by taking $\ell = \min(\ell_*, \ell_{\text{crit}})$. For other values of ℓ , the variance dominates and we have

$$E_{\text{test}}(\hat{w}_n^{\text{pred}}) \asymp T^{-(1-\ell/\beta)} + T^{-(b-\ell/\beta-a)} \asymp T^{-(\gamma-\ell/\beta)},$$

where $\gamma := \min(1, b-a)$. This is minimized by taking $\ell = \ell_{\text{crit}}$, leading to $E_{\text{test}}(\hat{w}_n^{\text{pred}}) \asymp T^{-(\gamma-1/(2\beta r+1))}$. This tends to zero with $T \rightarrow \infty$ only if $b > a + 1/(2\beta r + 1)$.

6. Experiments

We perform the following experiments on both simulated and real data to empirically validate our theoretical results.

6.1. Simulated Data

We consider ordinary / linear ridge regression in \mathbb{R}^d , for $d = 300$ and different structures for the covariance matrix Σ of the inputs: isotropic (i.e $\Sigma = I_d$) and power-law (30), with $(\beta, r) = (2, 0.375)$. For each value of n (the generation index), the fake data-generator is constructed according to the process described in (4). Then, for different values of T (between 1 and 1000,000), a sample of size T is drawn from this fake data-generator and then a downstream ridge model (7) is fitted. The test set consists of 100,000 clean pairs (x, y) form the true data distribution $P_{\Sigma, w_0, \sigma^2}$. This experiment is repeated 10 times to generate error bars. The results for the isotropic setting are shown in Figure 1 and the results for the power-law setting are shown in Figure 2. Figure 3 shows the over-parametrized setting.

6.2. Real Data: Kernel Ridge Regression on MNIST

As in Cui et al. (2022); Wei et al. (2022) we consider a distribution on MNIST, a popular dataset in the ML community. The classification dataset contains 60,000 training and 10,000 test data points (handwritten), with labels from

0 to 9 inclusive. Like in Cui et al. (2022), we convert the labels into real numbers (i.e a regression problem) as follows: $y = \text{label mod } 2 + \text{noise}$, where the variance of the noise is $\sigma^2 = 1$ (for simplicity, we also set $\sigma_0^2 = 1$). The test set consists of 10,000 pairs (x, y) , with the labels y constructed as described in the previous sentence. The fake data used for training is generated as in the previous experiment, but via kernel ridge regression (instead of least squares) with the RBF kernel (bandwidth = 10^{-4}) and the polynomial kernel (degree = 5, bandwidth = 10^{-3}). Note that it was empirically shown in Cui et al. (2022) that these datasets verify (30) with $(\beta, r) \approx (1.65, 0.097)$ in the case of the aforementioned RBF kernel, and $(\beta, r) \approx (1.2, 0.15)$ in the case of the polynomial kernel. Then, for different values of T (between 1 and 1000), a sample of size T is drawn from this fake data-generator and then a downstream kernel ridge model is fitted. Each of these experiments are repeated 10 times to generate error bars (due to different realizations of label noise). The results are shown in Figure 5.

7. Concluding Remarks

As we navigate the "synthetic data age", our findings signal a departure from traditional test error rates (e.g neural scaling laws), introducing novel challenges and phenomena with the integration of synthetic data from preceding AI models into training sets. Our work provides a solid analytical handle for demystifying the model collapse phenomenon as a modification of usual scaling laws caused by fake / synthesized training data.

A direct consequence of our multiplicative degradation result is that, over time (i.e as the number of generations becomes large), the effect of large language models (like ChatGPT) in the wild will be a pollution of the web to the extent that learning will be impossible. This will likely increase the value and cost of clean / non-AI-generated data.

On the practical side, our analysis reveals that AI-generated data alters the optimal regularization for downstream models. Drawing from the insight that regularization mirrors early stopping (Ali et al., 2019), our study suggests that models trained on mixed real and AI-generated data may initially improve but later decline in performance (model collapse), necessitating early detection of this inflection point. This observation prompts a re-evaluation of current training approaches and underscores the complexity of model optimization in the era of synthetic data.

References

- Achiam, J., Adler, S., Agarwal, S., Ahmad, L., Akkaya, I., Aleman, F. L., Almeida, D., Altenschmidt, J., Altman, S., Anadkat, S., et al. Gpt-4 technical report. *arXiv preprint arXiv:2303.08774*, 2023.
- Alemohammad, S., Casco-Rodriguez, J., Luzi, L., Humayun, A. I., Babaei, H., LeJeune, D., Siahkoochi, A., and Baraniuk, R. G. Self-consuming generative models go mad. *arXiv preprint arxiv:2307.01850*, 2023.
- Ali, A., Kolter, J. Z., and Tibshirani, R. J. A continuous-time view of early stopping for least squares regression. In Chaudhuri, K. and Sugiyama, M. (eds.), *Proceedings of the Twenty-Second International Conference on Artificial Intelligence and Statistics*, volume 89 of *Proceedings of Machine Learning Research*, pp. 1370–1378. PMLR, 16–18 Apr 2019.
- Bach, F. High-dimensional analysis of double descent for linear regression with random projections, 2023.
- Bai, Z. and Silverstein, J. W. J. W. *Spectral analysis of large dimensional random matrices*. Springer series in statistics. Springer, New York ;, 2nd ed. edition, 2010. ISBN 9781441906601.
- Belkin, M., Ma, S., and Mandal, S. To understand deep learning we need to understand kernel learning. In *Proceedings of the 35th International Conference on Machine Learning*, volume 80 of *Proceedings of Machine Learning Research*, pp. 541–549. PMLR, 2018.
- Berthier, R., Bach, F. R., and Gaillard, P. Tight nonparametric convergence rates for stochastic gradient descent under the noiseless linear model. *CoRR*, abs/2006.08212, 2020. URL <https://arxiv.org/abs/2006.08212>.
- Bertrand, Q., Bose, A. J., Duplessis, A., Jiralerspong, M., and Gidel, G. On the stability of iterative retraining of generative models on their own data. *arXiv preprint arxiv:2310.00429*, 2023.
- Bohacek, M. and Farid, H. Nepotistically trained generative-ai models collapse, 2023.
- Bordelon, B., Canatar, A., and Pehlevan, C. Spectrum dependent learning curves in kernel regression and wide neural networks. In *Proceedings of the 37th International Conference on Machine Learning, ICML 2020, 13-18 July 2020, Virtual Event*, volume 119 of *Proceedings of Machine Learning Research*, pp. 1024–1034. PMLR, 2020.
- Briesch, M., Sobania, D., and Rothlauf, F. Large language models suffer from their own output: An analysis of the self-consuming training loop, 2023.
- Brown, T., Mann, B., Ryder, N., Subbiah, M., Kaplan, J. D., Dhariwal, P., Neelakantan, A., Shyam, P., Sastry, G., Askell, A., Agarwal, S., Herbert-Voss, A., Krueger, G., Henighan, T., Child, R., Ramesh, A., Ziegler, D., Wu, J., Winter, C., Hesse, C., Chen, M., Sigler, E., Litwin, M., Gray, S., Chess, B., Clark, J., Berner, C., McCandlish, S., Radford, A., Sutskever, I., and Amodei, D. Language models are few-shot learners. In Larochelle, H., Ranzato, M., Hadsell, R., Balcan, M., and Lin, H. (eds.), *Advances in Neural Information Processing Systems*, volume 33, pp. 1877–1901. Curran Associates, Inc., 2020.
- Caponnetto, A. and de Vito, E. Optimal rates for the regularized least-squares algorithm. *Foundations of Computational Mathematics*, 7:331–368, 2007.
- Chizat, L., Oyallon, E., and Bach, F. On lazy training in differentiable programming. *Advances in neural information processing systems*, 32, 2019.
- Cui, H., Loureiro, B., Krzakala, F., and Zdeborova, L. Generalization error rates in kernel regression: The crossover from the noiseless to noisy regime. In Beygelzimer, A., Dauphin, Y., Liang, P., and Vaughan, J. W. (eds.), *Advances in Neural Information Processing Systems*, 2021.
- Cui, H., Loureiro, B., Krzakala, F., and Zdeborová, L. Generalization error rates in kernel regression: the crossover from the noiseless to noisy regime. *Journal of Statistical Mechanics: Theory and Experiment*, 2022(11):114004, nov 2022.
- Cui, H., Loureiro, B., Krzakala, F., and Zdeborová, L. Error scaling laws for kernel classification under source and capacity conditions. *Machine Learning: Science and Technology*, 4(3):035033, August 2023. ISSN 2632-2153.
- Devlin, J., Chang, M.-W., Lee, K., and Toutanova, K. Bert: Pre-training of deep bidirectional transformers for language understanding. *arXiv preprint arXiv:1810.04805*, 2018.
- Dohmatob, E., Feng, Y., Yang, P., Charton, F., and Kempe, J. A tale of tails: Model collapse as a change of scaling laws, 2024.
- Guo, Y., Shang, G., Vazirgiannis, M., and Clavel, C. The curious decline of linguistic diversity: Training language models on synthetic text, 2023.
- Hastie, T., Montanari, A., Rosset, S., and Tibshirani, R. J. Surprises in high-dimensional ridgeless least squares interpolation. *The Annals of Statistics*, 50(2), 2022.
- Hataya, R., Bao, H., and Arai, H. Will large-scale generative models corrupt future datasets? In *Proceedings of the IEEE/CVF International Conference on Computer Vision (ICCV)*, pp. 20555–20565, October 2023.

- Hoffmann, J., Borgeaud, S., Mensch, A., Buchatskaya, E., Cai, T., Rutherford, E., de Las Casas, D., Hendricks, L. A., Welbl, J., Clark, A., Hennigan, T., Noland, E., Millican, K., van den Driessche, G., Damoc, B., Guy, A., Osindero, S., Simonyan, K., Elsen, E., Rae, J. W., Vinyals, O., and Sifre, L. Training compute-optimal large language models, 2022.
- Jacot, A., Gabriel, F., and Hongler, C. Neural tangent kernel: Convergence and generalization in neural networks. In Bengio, S., Wallach, H., Larochelle, H., Grauman, K., Cesa-Bianchi, N., and Garnett, R. (eds.), *Advances in Neural Information Processing Systems*, volume 31. Curran Associates, Inc., 2018.
- Kaplan, J., McCandlish, S., Henighan, T., Brown, T. B., Chess, B., Child, R., Gray, S., Radford, A., Wu, J., and Amodei, D. Scaling laws for neural language models. *arXiv preprint arXiv:2001.08361*, 2020.
- Knowles, A. and Yin, J. Anisotropic local laws for random matrices. *Probability Theory and Related Fields*, 169(1): 257–352, 2017.
- Lee, J., Bahri, Y., Novak, R., Schoenholz, S. S., Pennington, J., and Sohl-Dickstein, J. Deep neural networks as gaussian processes. In *6th International Conference on Learning Representations, ICLR 2018, Vancouver, BC, Canada, April 30 - May 3, 2018, Conference Track Proceedings*. OpenReview.net, 2018.
- Liang, T. and Rakhlin, A. Just interpolate: Kernel “Ridgeless” regression can generalize. *The Annals of Statistics*, 48(3), 2020.
- Liu, Y., Ott, M., Goyal, N., Du, J., Joshi, M., Chen, D., Levy, O., Lewis, M., Zettlemoyer, L., and Stoyanov, V. Roberta: A robustly optimized bert pretraining approach. *arXiv preprint arXiv:1907.11692*, 2019.
- Maloney, A., Roberts, D. A., and Sully, J. A solvable model of neural scaling laws, 2022.
- Martínez, G., Watson, L., Reviriego, P., Hernández, J. A., Juárez, M., and Sarkar, R. Combining generative artificial intelligence (ai) and the internet: Heading towards evolution or degradation? *arXiv preprint arxiv: 2303.01255*, 2023a.
- Martínez, G., Watson, L., Reviriego, P., Hernández, J. A., Juárez, M., and Sarkar, R. Towards understanding the interplay of generative artificial intelligence and the internet. *arXiv preprint arxiv: 2306.06130*, 2023b.
- Marčenko, V. and Pastur, L. Distribution of eigenvalues for some sets of random matrices. *Math USSR Sb*, 1: 457–483, 01 1967.
- Midjourney. Midjourney ai, 2023. URL <https://www.midjourney.com/>.
- Mobahi, H., Farajtabar, M., and Bartlett, P. Self-distillation amplifies regularization in Hilbert space. In *Advances in Neural Information Processing Systems*, volume 33, pp. 3351–3361. Curran Associates, Inc., 2020.
- Neal, R. M. Priors for infinite networks. In *Bayesian Learning for Neural Networks*, pp. 29–53. Springer, New York, 1996.
- Nitanda, A. and Suzuki, T. Optimal rates for averaged stochastic gradient descent under neural tangent kernel regime. In *International Conference on Learning Representations*, 2021.
- Pillaud-Vivien, L., Rudi, A., and Bach, F. R. Statistical optimality of stochastic gradient descent on hard learning problems through multiple passes. In Bengio, S., Wallach, H. M., Larochelle, H., Grauman, K., Cesa-Bianchi, N., and Garnett, R. (eds.), *Advances in Neural Information Processing Systems 31: Annual Conference on Neural Information Processing Systems 2018*, pp. 8125–8135, 2018.
- Rahimi, A. and Recht, B. Weighted sums of random kitchen sinks: Replacing minimization with randomization in learning. In *Advances in Neural Information Processing Systems*. Curran Associates, Inc., 2008.
- Ramesh, A., Pavlov, M., Goh, G., Gray, S., Voss, C., Radford, A., Chen, M., and Sutskever, I. Zero-shot text-to-image generation. In Meila, M. and Zhang, T. (eds.), *Proceedings of the 38th International Conference on Machine Learning Research*, volume 139 of *Proceedings of Machine Learning Research*, pp. 8821–8831. PMLR, 18–24 Jul 2021.
- Richards, D., Mourta, J., and Rosasco, L. Asymptotics of ridge(less) regression under general source condition. In *Proceedings of The 24th International Conference on Artificial Intelligence and Statistics*, volume 130 of *Proceedings of Machine Learning Research*. PMLR, 2021.
- Rombach, R., Blattmann, A., Lorenz, D., Esser, P., and Ommer, B. High-resolution image synthesis with latent diffusion models. In *Proceedings of the IEEE/CVF Conference on Computer Vision and Pattern Recognition (CVPR)*, pp. 10684–10695, June 2022.
- Rudi, A. and Rosasco, L. Generalization properties of learning with random features. In *Advances in Neural Information Processing Systems*. Curran Associates Inc., 2017. ISBN 9781510860964.
- Schmidt-Hieber, J. Nonparametric regression using deep neural networks with relu activation function. *Annals of Statistics*, 48, 08 2017.

- Shumailov, I., Shumaylov, Z., Zhao, Y., Gal, Y., Papernot, N., and Anderson, R. The curse of recursion: Training on generated data makes models forget. *arXiv preprint arxiv:2305.17493*, 2023.
- Simon, J. B., Dickens, M., and DeWeese, M. R. Neural tangent kernel eigenvalues accurately predict generalization. 2021.
- Spigler, S., Geiger, M., and Wyart, M. Asymptotic learning curves of kernel methods: empirical data versus teacher–student paradigm. *Journal of Statistical Mechanics: Theory and Experiment*, 2020(12), 2020.
- Suzuki, T. Adaptivity of deep reLU network for learning in besov and mixed smooth besov spaces: optimal rate and curse of dimensionality. In *International Conference on Learning Representations*, 2019.
- Taori, R. and Hashimoto, T. B. Data feedback loops: model-driven amplification of dataset biases. ICML’23. JMLR.org, 2023.
- Touvron, H., Martin, L., Stone, K., Albert, P., Almahairi, A., Babaei, Y., Bashlykov, N., Batra, S., Bhargava, P., Bhosale, S., et al. Llama 2: Open foundation and fine-tuned chat models. *arXiv preprint arXiv:2307.09288*, 2023.
- Wei, A., Hu, W., and Steinhardt, J. More than a toy: Random matrix models predict how real-world neural representations generalize. In *Proceedings of the 39th International Conference on Machine Learning*, volume 162 of *Proceedings of Machine Learning Research*. PMLR, 2022.
- Williams, C. Computing with infinite networks. In Mozer, M., Jordan, M., and Petsche, T. (eds.), *Advances in Neural Information Processing Systems*, volume 9. MIT Press, 1996.

Appendix / Supplementary Material for Model Collapse Demystified: The Case of Regression

Contents

A. Exact Characterization of Test Error Under Model Collapse

A.1. Proof of Theorem 4.1 (Ridgeless Regression)

The proof is by induction on the number of generations n of fake data. For $n = 0$, we have

$$\begin{aligned} E_{test}(\widehat{w}_0^{pred}) &= \mathbb{E} \|\widehat{w}_0^{pred} - w_0\|_{\Sigma}^2 = \mathbb{E} \|\widehat{w}_0^{pred} - \widehat{w}_0\|_2^2 = \mathbb{E} \|(X_0^\top X_0)^{-1} X_0^\top E_0\|_2^2 \\ &= \sigma^2 \mathbb{E} \operatorname{tr}(X_0^\top X_0)^{-1} = \sigma^2 \frac{d}{T-d-1} \simeq \frac{\sigma^2 \phi}{1-\phi}, \end{aligned} \quad (34)$$

where $\phi := d/T \in (0, 1)$ and the last step has made use of Lemma A.1 below. This is a well-known result for the test error of linear regression in the under-parametrized regime, without any AI pollution (fake / synthesized training data).

Analogously, for $n = 1$ one computes the test error after the first generation of fake data as follows

$$\begin{aligned} E_{test}(\widehat{w}_1^{pred}) &= \mathbb{E} \|\widehat{w}_1^{pred} - w_0\|_{\Sigma}^2 = \mathbb{E} \|\widehat{w}_1^{pred} - \widehat{w}_0\|_2^2 = \mathbb{E} \|\widehat{w}_1^{pred} - \widehat{w}_1 + \widehat{w}_1 - \widehat{w}_0\|_2^2 \\ &= \mathbb{E} \|(X_0^\top X_0)^{-1} X_0 E_0 + \widehat{w}_0^{pred} - w_0\|_2^2 = \mathbb{E} \|w_0 - \widehat{w}_0^{pred}\|_2^2 + \mathbb{E} \|(X_0^\top X_0)^{-1} X_0^\top E_0\|_2^2 \\ &= E_{test}(\widehat{w}_0^{pred}) + \frac{\sigma_0^2 d}{T_0 - d - 1} \simeq \frac{\sigma^2 \phi}{1-\phi} + \frac{\sigma_0^2 \phi_0}{1-\phi_0}, \end{aligned}$$

where $\phi_0 = d/T_0 \in (0, 1)$. Continuing the induction on n , we obtain the result. \square

Lemma A.1. *Let X_0 be an $T_0 \times d$ random matrix with iid rows from $N(0, \Sigma)$. If $T_0 \geq d + 2$, then the empirical covariance matrix $\widehat{\Sigma}_0 := X_0^\top X_0 / T_0$ is invertible a.s and*

$$\mathbb{E} [\widehat{\Sigma}_0^{-1}] = \frac{T_0}{T_0 - d - 1} \Sigma^{-1}.$$

A.2. Proof of Theorem 4.3 (Ridge Regression + General Covariance)

A.2.1. REPRESENTATION OF \widehat{w}_n AND \widehat{w}_n^{pred}

We first obtain explicit formulae for the labelling vectors \widehat{w}_n used in the fake-data generation process (5). For any integer $m \geq 0$, define $P_m = X_m^\dagger X_m$, the orthogonal projection matrix onto the subspace of \mathbb{R}^d spanned by the rows of X_m .

Observe from (5) that

$$\begin{aligned}
 \hat{w}_n &= X_{n-1}^\dagger \bar{Y}_{n-1} = X_{n-1}^\dagger (X_{n-1} \hat{w}_{n-1} + E_{n-1}) = P_{n-1} \hat{w}_{n-1} + X_{n-1}^\dagger E_{n-1} \\
 &= P_{n-1} X_{n-2}^\dagger (X_{n-2} \hat{w}_{n-2} + E_{n-2}) + X_{n-1}^\dagger E_{n-1} \\
 &= P_{n-1} P_{n-2} \hat{w}_{n-2} + P_{n-1} X_{n-2}^\dagger E_{n-2} + X_{n-1}^\dagger E_{n-1} \\
 &\quad \vdots \\
 &= P_{n-1} P_{n-2} \dots P_0 w_0 + P_{n-1} P_{n-2} \dots P_1 X_1^\dagger E_1 + P_{n-1} P_{n-2} \dots P_2 X_2^\dagger E_2 + \dots \\
 &\quad \vdots \\
 &= P_{n-1} P_{n-2} \dots P_0 w_0 + \sum_{m=0}^{n-1} P_{n-1} P_{n-2} \dots P_m X_m^\dagger E_m.
 \end{aligned} \tag{35}$$

We get the following result.

Lemma A.2. *For any $n \geq 0$, the following formula holds*

$$\hat{w}_n = \begin{cases} w_0, & \text{if } n = 0, \\ Q_{n-1} w_0 + \sum_{m=0}^{n-1} \bar{Q}_{n-1,m} E_m, & \text{if } n \geq 1, \end{cases} \tag{36}$$

where $\bar{Q}_{k,m} := Q_{k,m} X_m^\dagger$, $Q_{k,m} := P_k P_{k-1} \dots P_m$ and $Q_k := Q_{k,0} = P_k P_{k-1} \dots P_0$. Moreover, $\hat{w}_n \in \text{Im } P_{n-1}$ as soon as $n \geq 1$.

In particular, under the simplifying condition (22), it holds that

$$\hat{w}_n = \begin{cases} w_0, & \text{if } n = 0, \\ P_0 w_0 + X_0^\dagger \bar{E}_{n-1} \in \text{Im } P_0, & \text{if } n \geq 1. \end{cases} \tag{37}$$

where $\bar{E}_{n-1} := \sum_{m=0}^{n-1} E_m$, a random vector of length T_0 , with iid entries from $N(0, n\sigma_0^2)$, and independent of X_0 . Moreover, $\hat{w}_n \in \text{Im } P_0$ as soon as $n \geq 1$.

Note that the second part of the result uses the elementary linear-algebraic fact that $P_m X_m^\dagger = X_m^\dagger$. In the special case where $T_0 \geq d$, we have $P_0 = I$ a.s., and so $\hat{w}_n = w_0 + X_0^\dagger \bar{E}_{n-1}$. Otherwise, even in the absence of generator noise ($\sigma_0 = 0$), the fake data labeller $\hat{w}_n = P_0 w_0$ drifts away from the truth w_0 , into a subspace of \mathbb{R}^d spanned by the rows of X_0 .

Next, let us obtain a decomposition for the downstream predictor \hat{w}_n^{pred} defined in (7). As usual, let $\widehat{\Sigma} := X^\top X/T$ be the empirical covariance matrix with resolvent $R = (\widehat{\Sigma} + \lambda I)^{-1}$, and observe that the downstream model writes

$$\begin{aligned}
 \hat{w}_n^{\text{pred}} &= R X^\top \bar{Y}_n(X)/T = R X^\top (X \hat{w}_n + E)/T \\
 &= R X^\top (X Q_{n-1} w_0 + X \sum_{m=0}^{n-1} \bar{Q}_{n-1,m} E_m + E)/T \\
 &= R \widehat{\Sigma} Q_{n-1} w_0 + R X^\top E/T + R \widehat{\Sigma} \sum_{m=0}^{n-1} \bar{Q}_{n-1,m} E_m.
 \end{aligned} \tag{38}$$

A.2.2. PROOF OF THEOREM 4.3

Using the decomposition (38) for the downstream model \widehat{w}_n^{pred} , we deduce that

$$\begin{aligned}
 E_{test}(\widehat{w}_n^{pred}) &= \mathbb{E} \|\widehat{w}_n^{pred} - w_0\|_{\Sigma}^2 = \mathbb{E} \|R\widehat{\Sigma}P_0w_0 + RX^{\top}E/T + R\widehat{\Sigma} \sum_{m=0}^{n-1} \overline{Q}_{n-1,m}E_m - w_0\|_{\Sigma}^2 \\
 &= \mathbb{E} \|R\widehat{\Sigma}P_0w_0 - w_0 + RX^{\top}E/T + R\widehat{\Sigma} \sum_{m=0}^{n-1} \overline{Q}_{n-1,m}E_m\|_{\Sigma}^2 \\
 &= \mathbb{E} \|R\widehat{\Sigma}P_0w_0 - w_0\|_{\Sigma}^2 + \mathbb{E} \|RX^{\top}E/T\|_{\Sigma}^2 + \mathbb{E} \|R\widehat{\Sigma} \sum_{m=0}^{n-1} \overline{Q}_{n-1,m}E_m\|_{\Sigma}^2 \\
 &= \widetilde{Bias} + Var + n\sigma_0^2\rho,
 \end{aligned} \tag{39}$$

where $\widehat{\Sigma} := X^{\top}X/T$, \widetilde{Bias} , Var , and ρ are as given in the theorem. On the second line, we have used independence (of X , X_0 , E , and \overline{E}_{n-1}) and the fact that E and \overline{E}_{n-1} are centered Gaussian random vectors, with iid components of variances σ^2 and $n\sigma_0^2$ respectively. \square

A.3. Proof of Theorem 4.6

Analysis of Bias-like Term. An exact analysis of the \widetilde{Bias} term appearing in Theorems 4.3 and 4.6 is presumably a treacherous enterprise given dependency on X (via R and $\widehat{\Sigma}$) and X_0 (via P_0). In place of such an analysis, we shall settle for the following result which gives an instructive lower-bound.

Proposition A.3. *In the RMT limit (17), it holds that*

$$\lim \widetilde{Bias} - \lim Bias \geq \lim \mathbb{E} \|R\widehat{\Sigma}P_0w_0 - R\widehat{\Sigma}w_0\|_{\Sigma}^2 \geq 0.$$

Thus, training on fake / synthesized data increases the bias term of the downstream model's test error !

Proof. Letting $A := R\widehat{\Sigma}$, one computes

$$\begin{aligned}
 \widetilde{Bias} - Bias &= \|AP_0w_0 - w_0\|_{\Sigma}^2 - \|Aw_0 - w_0\|_{\Sigma}^2 \\
 &= \|AP_0w_0 - Aw_0 + Aw - w\|_{\Sigma}^2 - \|Aw_0 - w_0\|_{\Sigma}^2 \\
 &= \|AP_0w_0 - Aw_0\|_{\Sigma}^2 + 2w_0^{\top}(A - P_0A)\Sigma(I - A)w_0 \\
 &= \|AP_0w_0 - Aw_0\|_{\Sigma}^2 + 2w_0^{\top}(I - P_0)A\Sigma(I - A)w_0.
 \end{aligned} \tag{40}$$

It then suffices to observe that, in the RMT limit (17), it holds that

$$\lim \mathbb{E} w_0^{\top}(I - P_0)A\Sigma(I - A)w_0 \geq 0,$$

as can be seen from repeated application of Propositions 1 and 2 of Bach (2023). \square

Analysis of ρ Term. Define a $d \times d$ random psd matrix $H := \widehat{\Sigma}R\Sigma\widehat{\Sigma}R$. Under the simplifying assumption (22), the matrices $\overline{Q}_{k,m}$ defined in the theorem all equal $\overline{Q}_{0,0} = X_0^{\dagger}$. It follows that the ρ -term in (12) then writes

$$\rho = \frac{1}{n} \sum_{m=0}^{n-1} \mathbb{E} [\overline{Q}_{n-1,m} \overline{Q}_{n-1,m}^{\top} H] = \mathbb{E} [\text{tr} X_0^{\dagger} (X_0^{\dagger})^{\top} H] = \mathbb{E}_H \mathbb{E} [\text{tr} X_0^{\dagger} (X_0^{\dagger})^{\top} H \mid H]. \tag{41}$$

Now, one computes the conditional expectation as follows

$$\begin{aligned}
 \mathbb{E} [\text{tr} X_0^{\dagger} (X_0^{\dagger})^{\top} H \mid H] &= \mathbb{E} [\text{tr} X_0^{\top} (X_0 X_0^{\top})^{-2} X_0 H \mid H] \\
 &= \lim_{\lambda_0 \rightarrow 0^+} \frac{1}{T_0} \frac{\partial}{\partial \lambda_0} \mathbb{E} [\text{tr} X_0^{\top} (X_0 X_0^{\top} + \lambda_0 T_0 I)^{-1} X_0 H \mid H].
 \end{aligned} \tag{42}$$

Furthermore, defining $A := \Sigma^{1/2}H\Sigma^{1/2}$ and $Z_0 = X_0\Sigma^{-1/2}$, we have

$$\begin{aligned}\text{tr } X_0^\top (X_0X_0^\top + \lambda_0 T_0 I)^{-1} X_0 H &= \text{tr } \Sigma^{1/2} Z_0^\top (Z_0 \Sigma Z_0^\top + \lambda_0 T_0 I)^{-1} Z_0 \Sigma^{1/2} H \\ &= \text{tr } A Z_0^\top (Z_0 \Sigma Z_0^\top + \lambda_0 T_0 I)^{-1} Z_0,\end{aligned}$$

We deduce from Proposition 2 of Bach (2023) that

$$\mathbb{E} [\text{tr } X_0^\top (X_0X_0^\top + \lambda_0 T_0 I)^{-1} X_0 H \mid H] \simeq \text{tr } A(\Sigma + \kappa(\lambda_0, T_0)I)^{-1} = \text{tr } H(\Sigma + \kappa(\lambda_0, T_0)I)^{-1}\Sigma. \quad (43)$$

Differentiating w.r.t. λ_0 and letting this parameter tend to zero from above gives

$$\begin{aligned}\mathbb{E} [\text{tr } X_0^\dagger (X_0^\dagger)^\top H \mid H] &= -\frac{1}{T_0} \lim_{\lambda_0 \rightarrow 0^+} \frac{\partial}{\partial \lambda_0} \mathbb{E} [\text{tr } X_0^\top (X_0X_0^\top + \lambda_0 T_0 I)^{-1} X_0 H \mid H] \\ &\simeq -\frac{1}{T_0} \lim_{\lambda_0 \rightarrow 0^+} \frac{\partial \kappa(\lambda_0, T_0)}{\partial \lambda_0} \cdot \frac{\partial}{\partial t} \text{tr } H(\Sigma + tI)^{-1}\Sigma \Big|_{t=\kappa(\lambda_0, T_0)} \simeq \frac{\text{tr } H(\Sigma + \kappa_0 I)^{-2}\Sigma}{T_0 - \text{df}_2(\kappa_0)},\end{aligned} \quad (44)$$

where $\kappa_0 = \kappa(0, T_0)$, and we have made use of Lemma C.2. Combining with (41) and then applying Proposition 1 of Bach (2023) to compute $\mathbb{E}_H \text{tr } H(\Sigma + \kappa_0 I)^{-2}\Sigma = \mathbb{E}_X \text{tr } \widehat{\Sigma} R \Sigma \widehat{\Sigma} R (\Sigma + \kappa_0 I)^{-2}\Sigma$ gives the following result.

Proposition A.4. *In the RMT limit (17), it holds for any $\lambda > 0$ that*

$$\rho = \frac{\text{tr } \Sigma^4 (\Sigma + \kappa_0 I)^{-2} (\Sigma + \kappa I)^{-2}}{T_0 - \text{df}_2(\kappa_0)} + \frac{\kappa^2 \text{tr } \Sigma^2 (\Sigma + \kappa_0 I)^{-2} (\Sigma + \kappa I)^{-2}}{T_0 - \text{df}_2(\kappa_0)} \cdot \frac{\text{df}_2(\kappa)}{T - \text{df}_2(\kappa)}, \quad (45)$$

where $\kappa_0 := \kappa(\lambda_0, T_0)$ and $\kappa = \kappa(\lambda, T)$.

In particular, if $T_0 \geq d$, then

$$\rho \simeq \frac{\text{df}_2(\kappa)}{T - \text{df}_2(\kappa)} \left(1 + \frac{\kappa^2 \text{tr}(\Sigma + \kappa I)^{-2}}{T_0 - \text{df}_2(\kappa_0)} \right). \quad (46)$$

This result completes the proof of Theorem 4.6. □

A.4. Proof of Corollary 4.7

For the first part, we know from Theorem 4.3 that

$$E_{test}(\widehat{w}_n^{pred}) = E_{test}(\widehat{w}_0^{pred}) + n\sigma_0^2 \rho, \text{ with} \quad (47)$$

$$\rho := \frac{\mathbb{E} \text{tr } \Sigma^{-1} \widehat{\Sigma} (\widehat{\Sigma} + \lambda I)^{-1} \Sigma (\widehat{\Sigma} + \lambda I)^{-1} \widehat{\Sigma}}{T_0 - d}. \quad (48)$$

The $E_{test}(\widehat{w}_0^{pred})$ term is taken care of by Proposition 4.5, since this corresponds to generalization error on clean training data. For the ρ term, we use Proposition 1 of Bach (2023) with $A = \Sigma^{-1}$ and $B = \Sigma$ to get

$$\begin{aligned}\rho &\simeq \frac{\text{tr}(\Sigma + \kappa I)^{-2}\Sigma^2}{T_0 - d} + \frac{\kappa^2 \text{tr}(\Sigma + \kappa I)^{-2}}{T_0 - d} \frac{\text{tr}(\Sigma + \kappa I)^{-2}\Sigma^2}{T - \text{df}_2(\kappa)} \\ &= \frac{\text{df}_2(\kappa)}{T_0 - d} + \frac{\kappa^2 \text{tr}(\Sigma + \kappa I)^{-2}}{T_0 - d} \frac{\text{df}_2(\kappa)}{T - \text{df}_2(\kappa)},\end{aligned}$$

which proves the first part of the result.

For the second part, note that $\text{df}_2(\kappa) = d/(1 + \kappa)^2$ when $\Sigma = I$, (15) holds, and so

$$\begin{aligned}(1 - 1/\phi_0)\rho &\simeq \frac{1}{(1 + \kappa)^2} + \frac{\kappa^2}{(1 + \kappa)^4} \frac{d}{T - d/(1 + \kappa)^2} \\ &\simeq \frac{1}{(1 + \kappa)^2} + \frac{\kappa^2}{(1 + \kappa)^4} \frac{\phi}{1 - \phi/(1 + \kappa)^2} \\ &= \frac{1}{(1 + \kappa)^2} + \frac{1}{(1 + \kappa)^2} \frac{\phi \kappa^2}{(1 + \kappa)^2 - \phi},\end{aligned}$$

and the result follows. □

A.5. A Note on Proposition 4.5

As mentioned in the main text, the result is classical Richards et al. (2021); Hastie et al. (2022); Bach (2023)). Only the second part needs a comment which we now provide. Indeed, the second part of the result follows from the first as we now see. Indeed, $w_0^\top \Sigma (\Sigma + \kappa I)^{-2} w_0 = r^2 / (1 + \kappa)^2$, $\text{df}_2(\kappa) = d / (1 + \kappa)^2$ and so we deduce from the first part that

$$\begin{aligned} \text{Var} &\simeq \sigma^2 \phi \frac{1}{(1 + \kappa)^2} \frac{1}{1 - \phi / (1 + \kappa)^2} = \frac{\sigma^2 \phi}{(1 + \kappa)^2 - \phi}, \\ \text{Bias} &\simeq \kappa^2 \|w_0\|_2^2 \frac{1}{(1 + \kappa)^2} \frac{1}{1 - \phi / (1 + \kappa)^2} = \frac{\kappa^2 \|w_0\|_2^2}{(1 + \kappa)^2 - \phi}, \end{aligned}$$

from which the result follows. \square

We now need to estimate $\delta^\top H \delta$ for a deterministic psd matrix H . Observe that

$$\begin{aligned} \delta^\top H \delta &= (Q_{n-1} w_0 - w_0)^\top H (Q_{n-1} w_0 - w_0) \\ &= w_0^\top Q_{n-1}^\top H Q_{n-1} w_0 - 2w_0^\top Q_{n-1}^\top H w_0 + w_0^\top H w_0. \end{aligned} \quad (49)$$

A.6. Proof of Theorem 4.8 and Theorem 4.9 (Model Collapse in the Absence of Label Noise)

We first prove Theorem 4.9. Note that since we are in the isotropic case, ΔBias defined in (20) is now given by $\Delta \text{Bias} := \mathbb{E} \|\widehat{\Sigma} R (Q_{n-1} w_0 - w_0)\|^2$, where $Q_{n-1} := P_{n-1} P_{n-2} \dots P_0$. Moreover, since $T > d$ and $\lambda = 0$ by assumption, we have $\Sigma R = I_d$, and so we further have $\Delta \text{Bias} := \mathbb{E} \|Q_{n-1} w_0 - w_0\|^2$. Now, one computes

$$\begin{aligned} \|Q_{n-1} w_0 - w_0\|^2 &= \|w_0\|^2 - 2w_0^\top Q_{n-1} w_0 + w_0^\top Q_{n-1}^\top Q_{n-1} w_0 \\ &= \|w_0\|^2 - w_0^\top Q_{n-1} w_0 \\ &\simeq \|w_0\|^2 - w_0^\top \left(\prod_{m=0}^{n-1} (I + \kappa_m I)^{-1} \right) w_0 \\ &= \|w_0\|^2 - \|w_0\|^2 \prod_{m=0}^{n-1} \min(1/\phi_m, 1), \end{aligned} \quad (50)$$

where on the 2nd line we have used the fact that $Q_{n-1}^\top Q_{n-1} = Q_{n-1}$ because the P_m 's are projections; on the 3rd line we have used Lemma A.5 with $\Sigma = I$ and $u = v = w_0$; on the 4th line we have used the fact that $\kappa_m := \kappa(0, T_m) = \max(\phi_m - 1, 0) = \max(\phi_m, 1) - 1$. This completes the proof of Theorem 4.9.

The proof of Theorem 4.8 is completely analogous, with Q_{n-1} replaced with Q_0 . \square

Lemma A.5. *Let X_0, \dots, X_{n-1} be independent random matrices of shapes $T_m \times d$ for $m = 0, \dots, n-1$, with rows iid from $N(0, \Sigma)$, and let $Q_{n-1} := P_{n-1} P_{n-2} \dots P_0$, where $P_m = X_m^\dagger X_m$ is the orthogonal projection onto the subspace of \mathbb{R}^d spanned by the rows of X_m . Then, in the limit $d, T_0, \dots, T_{n-1} \rightarrow \infty$ such that $d/T_0 \rightarrow \phi_0 \in (0, \infty), \dots, d/T_{n-1} \rightarrow \phi_{n-1} \in (0, \infty)$ with $\|\Sigma\|_{\text{op}}, \|\Sigma^{-1}\|_{\text{op}} = O(1)$, it holds that for deterministic L_2 -bounded sequences of vectors u and v*

$$u^\top Q_{n-1} v \simeq u^\top \left(\prod_{m=0}^{n-1} (\Sigma + \kappa_m I)^{-1} \right) v, \quad (51)$$

where $\kappa_m = \kappa(0, T_m)$ is as defined in (14).

Proof. The proof is by induction on $n \geq 1$. For $n = 1$, we have $Q_{n-1} = Q_0 = P_0$. Thus,

$$\begin{aligned} u^\top Q_0 v &= u^\top P_0 v = \lim_{t \rightarrow 0^+} u^\top X_0^\top (X_0 X_0^\top + tI)^{-1} X_0 v \\ &\simeq \lim_{t \rightarrow 0^+} u^\top (\Sigma + \kappa(t, T) I)^{-1} v = u^\top (\Sigma + \kappa_0 I)^{-1} v, \end{aligned} \quad (52)$$

where $\kappa_0 := \kappa(0, T)$ and we used Proposition 2 of Bach (2023) at the beginning of the 2nd line. Now, suppose the claim holds for n , and let's prove that it holds for $n + 1$. Indeed,

$$u^\top Q_n v = u^\top P_n Q_{n-1} v \simeq u^\top P_{n-1} \prod_{m=0}^{n-1} (\Sigma + \kappa_m)^{-1} v \simeq u^\top \prod_{m=0}^n (\Sigma + \kappa_m)^{-1} v,$$

where the second step is an application of the induction hypothesis with $P_n u$ in place of u . \square

The following lemma can be used to compute $\|Q_{n-1}w_0 - w_0\|_\Sigma^2$ in the case of anisotropic Σ .

Lemma A.6. *Under the hypothesis of Lemma A.5, it holds that*

$$u^\top Q_{n-1}v \simeq u^\top \Sigma^n \left(\prod_{m=0}^{n-1} (\Sigma + \kappa_m I)^{-1} \right) v, \quad (53)$$

$$u^\top Q_{n-1}^\top \Sigma Q_{n-1}v \simeq u^\top \Sigma^n \left(\prod_{m=0}^{n-1} A_m \right) v, \text{ with } A_m := (\Sigma + \kappa_m I)^{-2} \left(\Sigma^2 + \frac{\kappa_m^2 \text{df}_2(\kappa_m)}{T - \text{df}_2(\kappa_m)} I \right), \quad (54)$$

where $\kappa_m := \kappa(0, T_m)$ as defined in (14).

Proof. The first formula follows directly from Lemma A.5 with u replaced with Σu . For the second formula, we can write

$$u^\top Q_{n-1}^\top M Q_{n-1}v = u^\top P_0 P_1 \dots P_{n-2} P_{n-1} M P_{n-1} P_{n-2} \dots P_0 P_1 v = \tilde{u}_{n-1}^\top P_{n-1} M P_{n-1} \tilde{v}_{n-1},$$

where $\tilde{u}_{n-1} := P_{n-2} \dots P_0 u$. So we really only need to prove the result for $n = 1$; the general case will follow by induction and due to multiplicativity. Indeed, defining $A = \Sigma^{1/2} u v^\top \Sigma^{1/2}$, $B = \Sigma^{1/2} M \Sigma^{1/2}$, and $Z_0 = X_0 \Sigma^{-1/2}$, we have

$$\begin{aligned} u^\top P_0 M P_0 v &= \lim_{t \rightarrow 0^+} u^\top X_0^\top (X_0 X_0^\top + tI)^{-1} X_0 M X_0^\top (X_0 X_0^\top + tI)^{-1} X_0 v \\ &= \lim_{t \rightarrow 0^+} \text{tr} A Z_0 (Z_0 \Sigma Z_0^\top + tI)^{-1} Z_0 B Z_0^\top (Z_0 Z_0^\top + tI)^{-1} Z_0 \\ &\simeq \text{tr} A (\Sigma + \kappa_0 I)^{-1} B (\Sigma + \kappa_0 I)^{-1} + \kappa_0^2 \text{tr} A (\Sigma + \kappa_0 I)^{-2} \cdot \frac{\text{tr} B (\Sigma + \kappa_0 I)^{-2}}{T - \text{df}_2(\kappa_0)} \\ &= u^\top (\Sigma + \kappa_0 I)^{-1} \Sigma M \Sigma (\Sigma + \kappa_0 I)^{-1} v + \kappa_0^2 u^\top \Sigma (\Sigma + \kappa_0 I)^{-2} v \cdot \frac{\text{tr} M \Sigma (\Sigma + \kappa_0)^{-2}}{T - \text{df}_2(\kappa_0)} \\ &= u^\top \Sigma A_0 v, \text{ for } M = \Sigma, \end{aligned} \quad (55)$$

where the 3rd line is an application of Proposition 2 of Bach (2023). \square

B. Proof of Results for Power-Law Covariance Spectrum

B.1. Proof of Theorem 5.2

From Theorem 4.3, we need to analyze the quantity

$$\rho \simeq \frac{\text{df}_2(\kappa(\lambda))}{T_0 - d} + \frac{\kappa(\lambda)^2 \text{tr} (\Sigma + \kappa(\lambda) I_d)^{-2}}{T_0 - d} \cdot \frac{\text{df}_2(\kappa(\lambda))}{T - \text{df}_2(\kappa(\lambda))}. \quad (56)$$

Now, for small λ , $\kappa := \kappa(\lambda)$ is small and one can compute

$$\text{df}_m(\kappa) \asymp \sum_i \frac{\lambda_i^m}{(\lambda_i + \kappa)^m} = \kappa^{-m} \sum_i \frac{\lambda_i^m}{(1 + \kappa^{-1} \lambda_i)^m} \asymp \kappa^{-m} \kappa^{(m-1/\beta)} = \kappa^{-1/\beta}, \quad (57)$$

where we have used Lemma C.1 with $D = \kappa^{-1}$ and $n = m$ in the last step. On the other hand, we can use some of the results of Appendix A (Section 3) of (Cui et al., 2022) to do the following. It can be shown (see aforementioned paper) that

- If $\ell > \beta$, then $\kappa \asymp T^{-\beta}$, and so $\text{df}_m(\kappa) \asymp T$ for all $m \geq 1$.
- If $\ell < \beta$, then $\kappa \asymp \lambda \asymp T^{-\ell}$, and so $\text{df}_m(\kappa) \asymp T^{\ell/\beta} = o(T)$ for all $m \geq 1$.

For $\ell < \beta$, plugging this into (56) gives

$$\begin{aligned} \rho &\asymp \frac{T^{\ell/\beta}}{T_0 - d} + \frac{d}{T_0 - d} \frac{T^{\ell/\beta}}{T - T^{\ell/\beta}} \asymp T_0^{-1} T^{\ell/\beta} + \frac{\phi_0}{1 - \phi_0} T^{-(1-\ell/\beta)} \\ &\asymp \frac{1}{1 - \phi_0} \max(T/T_0, \phi_0) T^{-(1-\ell/\beta)}, \end{aligned} \quad (58)$$

where $\phi_0 := d/T_0$. Combining our Theorem 4.3 with (63), we get the claimed result. \square

B.2. Representation of Clean Test Error

We make a small digression to present the following curiosity: with a slight leap of faith, the main results of (Cui et al., 2022) can be obtained in a few lines from the tools developed in (Bach, 2023), namely Proposition 4.5. This is significant, because the computations in (Cui et al., 2022) were done via methods of statistical physics (replica trick), while (Bach, 2023) is based on RMT.

Indeed, for regularization parameter $\lambda \asymp T^{-\ell}$ given in (31), we have $\kappa = \kappa(\lambda) \simeq \lambda$. Thus

$$\kappa \asymp T^{-\ell}, \quad \text{df}_2(\kappa) \asymp \kappa^{-1/\beta} \asymp T^{\ell/\beta}. \quad (59)$$

Now, since $\lambda_i \asymp i^{-\beta}$ (capacity condition) and $(w_0^\top v_i)^2 = c_i^2 \asymp i^{-\delta}$ (source condition), we deduce

$$\begin{aligned} \kappa^2 w_0^\top \Sigma (\Sigma + \kappa I)^{-2} w_0 &\asymp w_0^\top \left(\sum_i \frac{\lambda_i}{(\lambda_i + \kappa^{-1} \lambda_i)^2} v_i v_i^\top \right) w_0 = \sum_i \frac{c_i^2 \lambda_i}{(\lambda_i + \kappa^{-1} \lambda_i)^2} \\ &= \sum_i \frac{c_i^2 \lambda_i}{(\lambda_i + \kappa^{-1} \lambda_i)^2} \asymp \sum_i \frac{\lambda_i^{1+\delta/\beta}}{(\lambda_i + \kappa^{-1} \lambda_i)^2} \asymp \kappa^{-\gamma} \asymp T^{-\ell\gamma}, \end{aligned} \quad (60)$$

where $\gamma = \min(2, 1 + \delta/\beta - 1/\beta) = \min(2, 2r) = 2\underline{r}$, with $\underline{r} := \min(r, 1)$. The exponent is so because $\delta = 1 + \beta(2r - 1)$, and so $\delta/\beta = 1/\beta + 2r - 1$ by construction. The estimation of the last sum in (60) is thanks to Lemma C.1 applied with $D = \kappa^{-1}$, $n = 1 + \delta/\beta$, and $m = 2$. Therefore, invoking Proposition 4.5 gives

$$\text{Bias} \simeq \frac{\kappa^2 w_0^\top \Sigma (\Sigma + \kappa)^{-2} w_0}{1 - \text{df}_2(\kappa)/T} \asymp \frac{T^{\ell\gamma}}{1 - T^{-(1-\ell/\beta)}} \asymp T^{-\ell\gamma} = T^{-2\underline{r}\ell} \quad (61)$$

$$\text{Var} \simeq \sigma^2 \frac{\text{df}_2(\kappa)}{T} \cdot \frac{1}{1 - \text{df}_2(\kappa)/T} \asymp \sigma^2 \frac{T^{\ell/\beta}}{T} \frac{1}{1 - o(1)} \asymp \sigma^2 T^{-(1-\ell/\beta)}. \quad (62)$$

We deduce the scaling law

$$E_{\text{test}} \simeq \text{Bias} + \text{Var} \asymp T^{-2\underline{r}\ell} + \sigma^2 T^{-(1-\ell/\beta)} \asymp \max(\sigma^2, T^{1-2\underline{r}\ell-\ell/\beta}) T^{-(1-\ell/\beta)}, \quad (63)$$

which is precisely the main result of (Cui et al., 2022).

Low-Noise Regime. In the low noise regime where $\sigma^2 = O(T^{-2\beta\underline{r}})$, one may take $\ell = \beta$; the variance is then much smaller than the bias, and one has the fast rate

$$E_{\text{test}} \asymp T^{-2\beta\underline{r}}. \quad (64)$$

High-Noise Regime. Now, consider the case where $\sigma^2 = \Theta(1)$. Setting $2\underline{r}\ell = 1 - \ell/\beta$ to balance out the bias and variance gives $\ell = \ell_{\text{crit}}$, where

$$\ell_{\text{crit}} := \frac{\beta}{2\beta\underline{r} + 1} \in (0, \beta). \quad (65)$$

With this value of the exponent ℓ , we get the error rate

$$E_{\text{test}} \asymp T^{-2\ell_{\text{crit}}\underline{r}} = T^{-c}, \quad \text{with } c := \frac{2\beta\underline{r}}{2\beta\underline{r} + 1}, \quad (66)$$

which is precisely the main result of (Cui et al., 2022), known to be minimax optimal (de Vito (Caponnetto & de Vito, 2007), etc.) !

C. Auxiliary Lemmas

Lemma C.1. *Let the sequence $(\lambda_k)_{k \geq 1}$ of positive numbers be such that $\lambda_k \asymp k^{-\beta}$ for some constant $\beta > 0$, and let $m, n \geq 0$ with $n\beta > 1$. Then, for $D \gg 1$, it holds that*

$$\sum_{k=1}^{\infty} \frac{\lambda_k^n}{(1 + D\lambda_k)^m} \asymp D^{-c} \begin{cases} \log D, & \text{if } m = n - 1/\beta, \\ 1, & \text{else,} \end{cases} \quad (67)$$

where $c := \min(m, n - 1/\beta) \geq 0$.

Proof. First observe that

$$\begin{aligned} \lambda_k^n / (1 + D\lambda_k)^m &\asymp \lambda_k^n \min(1, (D\lambda_k)^{-m}) \\ &= \begin{cases} \lambda_k^n = k^{-n\beta}, & \text{if } D\lambda_k < 1, \text{ i.e if } k > D^{1/\beta}, \\ D^{-m} \lambda_k^{-(m-n)} = D^{-m} k^{(m-n)\beta}, & \text{else.} \end{cases} \end{aligned}$$

We deduce that

$$\sum_{k=1}^{\infty} \frac{\lambda_k^n}{(1 + D\lambda_k)^m} \asymp D^{-m} \sum_{1 \leq k \leq D^{1/\beta}} k^{(m-n)\beta} + \sum_{k > D^{1/\beta}} k^{-n\beta}. \quad (68)$$

By comparing with the corresponding integral, one can write the first sum in (68) as

$$\begin{aligned} D^{-m} \sum_{1 \leq k \leq D^{1/\beta}} k^{(m-n)\beta} &\asymp D^{-m} \int_1^{D^{1/\beta}} u^{(m-n)\beta} du \\ &\asymp D^{-m} \begin{cases} (D^{1/\beta})^{1+(m-n)\beta} = D^{-(n-1/\beta)}, & \text{if } n - 1/\beta < m, \\ \log D, & \text{if } m = n - 1/\beta, \\ 1, & \text{else.} \end{cases} \\ &= \begin{cases} D^{-(n-1/\beta)}, & \text{if } n - 1/\beta < m, \\ D^{-m} \log D, & \text{if } m = n - 1/\beta, \\ D^{-m}, & \text{else.} \end{cases} \\ &= D^{-c} \begin{cases} \log D, & \text{if } m = n - 1/\beta, \\ 1, & \text{else,} \end{cases} \end{aligned}$$

where $c \geq 0$ is as given in the lemma.

Analogously, one can write the second sum in (68) as

$$\sum_{k > D^{1/\beta}} k^{-n\beta} \asymp \int_{D^{1/\beta}}^{\infty} u^{-n\beta} du \asymp (D^{1/\beta})^{1-n\beta} = D^{-(n-1/\beta)},$$

and the result follows upon putting things together. \square

Lemma C.2. For $\kappa = \kappa(\lambda, T)$ defined as in (14), it holds that

$$\frac{\partial \kappa}{\partial \lambda} = \frac{1}{1 - \text{df}_2(\kappa)/T} \geq 1. \quad (69)$$

Thus, perhaps more conveniently, this lemma allows us to rewrite

$$\text{Bias} = w_0^\top \Sigma (\Sigma + \kappa I)^{-2} w_0 \frac{\partial \kappa}{\partial \lambda}, \quad (70)$$

$$\text{Var} = \sigma^2 \frac{\text{df}_2(\kappa)}{T} \frac{\partial \kappa}{\partial \lambda}. \quad (71)$$

The RHS of (70) is usually referred to as the omniscient risk Hastie et al. (2022); Cui et al. (2021); Wei et al. (2022).

Proof of Lemma C.2. By definition of κ , we know that

$$\kappa - \lambda = \kappa \text{df}_1(\kappa)/T = \kappa \text{tr} \Sigma (\Sigma + \kappa I)^{-1}/T.$$

Differentiating w.r.t. λ gives

$$\kappa' - 1 = \kappa' (\text{tr} \Sigma (\Sigma + \kappa I)^{-1} - \kappa \text{tr} \Sigma (\Sigma + \kappa)^{-2})/T = \kappa' \text{tr} \Sigma^2 (\Sigma + \kappa I)^{-2}/T = \kappa' \text{df}_2(\kappa)/T,$$

and the result follows upon rearranging. Note that we have used the identity

$$I - \kappa(\Sigma + \kappa I)^{-1} = \Sigma(\Sigma + \kappa I)^{-1},$$

to rewrite $\Sigma(\Sigma + \kappa I)^{-1} - \kappa\Sigma(\Sigma + \kappa I)^{-2} = \Sigma^2(\Sigma + \kappa I)^{-2}$.

□